

Effects of hydrologic conditions on SWAT model performance and parameter sensitivity for a small, mixed land use catchment in New Zealand

W. Me^{1,2}, J. M. Abell^{1,*}, D. P. Hamilton¹

[1]{Environmental Research Institute, University of Waikato, Private Bag 3105, Hamilton 3240, New Zealand}

[2]{College of Hydrology and Water Resources, Hohai University, Nanjing, 210098, People's Republic of China}

[*]{now at: Ecofish Research Ltd., Suite 1220 – 1175 Douglas Street, Victoria, British Columbia, Canada}

Correspondence to: W. Me (yaowang0418@gmail.com)

Abstract

The Soil Water Assessment Tool (SWAT) was configured for the Puarenga Stream catchment (77 km²), Rotorua, New Zealand. The catchment land use is mostly plantation forest, some of which is spray-irrigated with treated wastewater. A Sequential Uncertainty Fitting (SUFI-2) procedure was used to auto-calibrate unknown parameter values in the SWAT model. Model validation was performed using two datasets: 1) monthly instantaneous measurements of suspended sediment (SS), total phosphorus (TP) and total nitrogen (TN) concentrations; and 2) high-frequency (1–2 h) data measured during rainfall events. Monthly instantaneous TP and TN concentrations were generally not reproduced well (24% bias for TP, 27% bias for TN, and $R^2 < 0.1$, $NSE < 0$ for both TP and TN), in contrast to SS concentrations ($< 1\%$ bias; R^2 and NSE both > 0.75) during model validation. Comparison of simulated daily mean SS, TP and TN concentrations with daily mean discharge-weighted high-frequency measurements during storm events indicated that model predictions during the high rainfall period considerably underestimated concentrations of SS (44% bias) and TP (70% bias), while TN concentrations were comparable ($< 1\%$ bias; R^2 and NSE both ~ 0.5). This comparison highlighted the potential for model error associated with quick-

1 flow fluxes in flashy lower-order streams to be underestimated compared with
2 low-frequency (e.g. monthly) measurements derived predominantly from base
3 flow measurements. To address this, we recommend that high-frequency, event-
4 based monitoring data are used to support calibration and validation. Simulated
5 discharge, SS, TP and TN loads were partitioned into two components (base flow
6 and quick flow) based on hydrograph separation. A manual procedure (one-at-a-
7 time sensitivity analysis) was used to quantify parameter sensitivity for the two
8 hydrologically-separated regimes. Several SWAT parameters were found to have
9 different sensitivities between base flow and quick flow. Parameters relating to
10 main channel processes were more sensitive for the base flow estimates, while
11 those relating to overland processes were more sensitive for the quick flow
12 estimates. This study has important implications for identifying uncertainties in
13 parameter sensitivity and performance of hydrological models applied to
14 catchments with large fluctuations in stream flow, and in cases where models are
15 used to examine scenarios that involve substantial changes to the existing flow
16 regime.

17

18 **1 Introduction**

19 Catchment models are valuable tools for understanding natural processes
20 occurring at basin scales and for simulating the effects of different management
21 regimes on soil and water resources (e.g. Cao et al., 2006). Model applications
22 may have uncertainties as a result of errors associated with the forcing variables,
23 measurements used for calibration, and conceptualisation of the model itself
24 (Lindenschmidt et al., 2007). The ability of catchment models to simulate
25 hydrological processes and pollutant loads can be assessed through analysis of
26 uncertainty or errors during a calibration process that is specific to the application
27 domain (White and Chaubey, 2005).

28 The Soil and Water Assessment Tool (SWAT) model is increasingly used
29 to predict discharge, sediment and nutrient loads on a temporally resolved basis,
30 and to quantify material fluxes from a catchment to the downstream receiving
31 environment such as a lake (e.g. Nielsen et al., 2013). The SWAT model is
32 physically-based and provides distributed descriptions of hydrologic processes at
33 sub-basin scale (Arnold et al., 1998; Neitsch et al., 2011). It has numerous

1 parameters, some of which can be fixed on the basis of pre-existing catchment
2 data (e.g. soil maps) or knowledge gained in other studies. However, values for
3 other parameters need to be assigned during a calibration process as a result of
4 complex spatial and temporal variations that are not readily captured either
5 through measurements or within the model algorithms themselves (Boyle et al.,
6 2000). Such parameter values assigned during calibration are therefore lumped,
7 i.e., they integrate variations in space and/or time and thus provide an
8 approximation for real values which often vary widely within a study catchment.
9 Model calibration is an iterative process whereby parameters are adjusted to the
10 system of interest by refining model predictions to fit closely with observations
11 under a given set of conditions (Moriasi et al., 2007). Manual calibration depends
12 on the system used for model application, the experience of the modellers, and
13 knowledge of the model algorithms. It tends to be subjective and time-consuming.
14 By contrast, auto-calibration provides a less labour-intensive approach by using
15 optimisation algorithms (Eckhardt and Arnold, 2001). The Sequential Uncertainty
16 Fitting (SUFI-2) procedure has previously been applied to auto-calibrate
17 discharge parameters in a SWAT application for the Thur River, Switzerland
18 (Abbaspour et al., 2007), as well as for groundwater recharge, evapotranspiration
19 and soil storage water considerations in West Africa (Schuol et al., 2008). Model
20 validation is subsequently performed using measured data that are independent of
21 those used for calibration (Moriasi et al., 2007).

22 Values for hydrological parameter values in the SWAT model can vary
23 temporally. Cibin et al. (2010) found that the optimum calibrated values for
24 hydrological parameters varied with different flow regimes (low, medium and
25 high), thus suggesting that SWAT model performance can be optimised by
26 assigning parameter values based on hydrological characteristics. Other work has
27 similarly demonstrated benefits from assigning separate parameter values to low,
28 medium, and high discharge periods (Yilmaz et al., 2008), or based on whether a
29 catchment is in a dry, drying, wet or wetting state (Choi and Beven, 2007). Such
30 temporal dependence of model parameterisation on hydrologic conditions has
31 implications for model performance. Krause et al. (2005) compared different
32 statistical metrics of hydrological model performance separately for base-flow
33 periods and storm events to evaluate the performance. The authors found that the
34 logarithmic form of the Nash-Sutcliffe efficiency (NSE) value provided more

1 information on the sensitivity of model performance for discharge simulations
2 during storm events, while the relative form of NSE was better for base flow
3 periods. Similarly, Guse et al. (2014) investigated temporal dynamics of
4 sensitivity of hydrological parameters and SWAT model performance using
5 Fourier amplitude sensitivity test (Reusser et al., 2011) and cluster analysis
6 (Reusser et al., 2009). The authors found that three groundwater parameters were
7 highly sensitive during quick flow, while one evaporation parameter was most
8 sensitive during base flow, and model performance was also found to vary
9 significantly for the two flow regimes. Zhang et al. (2011) calibrated SWAT
10 hydrological parameters for periods separated on the basis of six climatic indexes.
11 Model performance improved when different values were assigned to parameters
12 based on six hydroclimatic periods. Similarly, Pfannerstill et al. (2014) found that
13 assessment of model performance was improved by considering an additional
14 performance statistic for very low-flow simulations amongst five hydrologically-
15 separated regimes.

16 To date, analysis of temporal dynamics of SWAT parameters has
17 predominantly focussed on simulations of discharge rather than water quality
18 constituents. This partly reflects the paucity of comprehensive water quality data
19 for many catchments; near-continuous discharge data can readily be collected but
20 this is not the case for water quality parameters such as suspended sediment or
21 nutrient concentrations. Data collected in monitoring programmes that involve
22 sampling at regular time intervals (e.g. monthly) are often used to calibrate water
23 quality models, but these are unlikely to fully represent the range of hydrologic
24 conditions in a catchment (Bieroza et al., 2014). In particular, water quality data
25 collected during storm-flow periods are rarely available for SWAT calibration,
26 thus prohibiting opportunities to investigate how parameter sensitivity varies
27 under conditions which can contribute disproportionately to nutrient or sediment
28 transport, particularly in lower-order catchments (Chiwa et al., 2010; Abell et al.,
29 2013). Failure to fully consider storm-flow processes could therefore result in
30 overestimation of model performance. Thus, further research is required to
31 examine how water quality parameters vary during different flow regimes and to
32 understand how model uncertainty may vary under future climatic conditions that
33 affect discharge regimes (Brigode et al., 2013).

1 In this study, the SWAT model was configured to a relatively small, mixed
2 land use catchment in New Zealand that has been the subject of an intensive water
3 quality sampling programme designed to target a wide range of hydrologic
4 conditions. A catchment-wide set of parameters was calibrated using the SUFI-2
5 procedure which is integrated into the SWAT Calibration and Uncertainty
6 Program (SWAT-CUP). The objectives of this study were to: (1) quantify the
7 performance of the model in simulating discharge and fluxes of suspended
8 sediments and nutrients at the catchment outlet; (2) rigorously evaluate model
9 performance by comparing daily simulation output with monitoring data collected
10 under a range of hydrologic conditions; and (3) quantify whether parameter
11 sensitivity varies between base flow and quick flow conditions.

13 **2 Methods**

14 **2.1 Study area**

15 The Puarenga Stream is the second-largest surface inflow to Lake Rotorua (Bay
16 of Plenty, New Zealand) and drains a catchment of 77 km². The catchment is
17 situated in the central North Island of New Zealand, which has a warm temperate
18 climate. Annual mean temperature at Rotorua Airport (Fig. 1a) is 15±4 °C and
19 annual mean evapotranspiration is 714 mm yr⁻¹ (1993–2012; National Climatic
20 Data Centre; available at <http://cliflo.niwa.co.nz/>). Annual mean precipitation at
21 Kaituna rain gauge (Fig. 1a) is 1500 mm yr⁻¹ (1993–2012; Bay of Plenty Regional
22 Council). The catchment is relatively steep (mean slope = 9%; Bay of Plenty
23 Regional Council) with predominantly pumice soils that have high macroporosity,
24 resulting in high infiltration rates and substantial sub-surface lateral flow
25 contributions to stream channels. Two cold-water springs (Waipa Spring and
26 Hemo Spring) and one geothermal spring (Fig. 1b) are located in the LTS. Two
27 cold-water springs have annual mean discharge of ~0.19 m³ s⁻¹ (Rotorua District
28 Council) and one geothermal spring has annual mean discharge of ~0.12 m³ s⁻¹
29 (White et al., 2004).

30 The predominant land use (47%) is exotic forest (*Pinus radiata*).
31 Approximately 26% is managed pastoral farmland, 11% mixed scrub and 9%
32 indigenous forest. Since 1991, treated wastewater has been pumped from the
33 Rotorua Wastewater Treatment Plant and spray-irrigated over 16 blocks of total

1 area of 1.93 km² in the Whakarewarewa Forest (Fig. 1a). Following this, it took
2 approximately four years before elevated nitrate concentrations were measured in
3 the receiving waters of the Puarenga Stream (Lowe et al., 2007). Prior to 2002, the
4 irrigation schedule entailed applying wastewater to two blocks per day so that
5 each block was irrigated approximately weekly. Since 2002, 10 to 14 blocks have
6 been irrigated simultaneously at daily frequency. Over the entire period of
7 irrigation, nutrient concentrations in the irrigated water have gradually decreased
8 as improvements in treatment of the wastewater have been made (Lowe et al.,
9 2007).

10 Measurements from the Forest Research Institute (FRI) stream–gauge (1.7
11 km upstream of Lake Rotorua; Fig. 1b) were considered representative of the
12 downstream/outlet conditions of the Puarenga Stream. The FRI stream–gauge was
13 closed in mid 1997, then reopened late in 2004 (Environment Bay of Plenty,
14 2007). Annual mean discharge at this site is 2.0 m³ s⁻¹ (1994–1997 and 2004–
15 2008; Bay of Plenty Regional Council). The Puarenga Stream receives a high
16 proportion of flow from groundwater stores and has only moderate seasonality in
17 discharge. On average, the lowest mean daily discharge is during summer
18 (December to February; 1.7 m³ s⁻¹) and the highest mean daily discharge is during
19 winter (June to August; 2.4 m³ s⁻¹). Discharge records during 1998–2004 were
20 intermittent and this precluded a detailed comparison of measured and simulated
21 discharge during that period. In July 2010, the gauge was repositioned 720 m
22 downstream to the State Highway 30 (SH 30) bridge (Fig. 1b).

23 **2.2 Model configuration**

24 SWAT input data requirements included a digital elevation model (DEM),
25 meteorological records, records of springs and water abstraction, soil
26 characteristics, land use classification, and management schedules for key land
27 uses (pastoral farming, wastewater irrigation, and timber harvesting). The SWAT
28 model version used (SWAT2009_rev488) runs on a daily time step.

29 The DEM was used to delineate boundaries of the whole catchment and
30 individual sub–catchments, with a stream map used to ‘burn–in’ channel locations
31 to create accurate flow routings. Hourly rainfall estimates were used as hydrologic
32 forcing data. The Penman–Monteith method (Monteith, 1965) was used to
33 calculate evapotranspiration (ET) and potential ET. The Green and Ampt (1911)

1 method was used to calculate infiltration, rather than the SCS curve number
2 method. Therefore, the hourly rainfall/Green & Ampt infiltration/daily routing
3 method (Neitsch et al., 2011) was chosen to simulate upland and in-stream
4 processes. Ten sub-catchments were represented in the Puarenga Stream
5 catchment, each comprising numerous Hydrologic Response Units (HRUs). Each
6 HRU aggregates cells with the same combination of land cover, soil, and slope. A
7 total of 404 HRUs was defined in the model. Runoff and nutrient transport were
8 predicted separately within SWAT for each HRU, with predictions summed to
9 obtain the total for each sub-catchment.

10 Descriptions and sources of the data used to configure the SWAT model
11 are given in Table 1. There were a total of 197 model parameters. Values of
12 SWAT parameters were assigned based on: i) measured data (e.g. some of the soil
13 parameters; Table 1); ii) literature values from published studies of similar
14 catchments (e.g. parameters for dominant land uses; Table 2); or iii) by calibration
15 where parameters were not otherwise prescribed.

16 SWAT simulates loads of ‘mineral phosphorus’ (MINP) and ‘organic
17 phosphorus’ (ORGP) of which the sum is total phosphorus (TP). The MINP
18 fraction represents soluble P either in mineral or in organic form, while ORGP
19 refers to particulate P bound either by algae or by sediment (White et al., 2014).
20 Soluble P may be taken up during algae growth, or released from benthic
21 sediment. Either fraction can be transformed to particulate P contained in algae or
22 sediment.

23 SWAT simulates loads of nitrate–nitrogen ($\text{NO}_3\text{-N}$), ammonium–nitrogen
24 ($\text{NH}_4\text{-N}$) and organic nitrogen (ORGN), the sum of which is total nitrogen (TN).
25 Nitrogen parameters were auto-calibrated for each N fraction. The SWAT model
26 does not account for the initial nitrate concentration in shallow aquifers, as also
27 noted by Conan et al. (2003). Ekanayake and Davie (2005) indicated that SWAT
28 underestimated N loading from groundwater and suggested a modification by
29 adding a background concentration of nitrate in streamflow to represent
30 groundwater nitrate contributions. Over the period of the first five years of
31 wastewater irrigation, nitrate concentrations in shallow groundwater draining the
32 Waipa Stream sub-catchment were estimated to have increased by c. 0.44 mg L^{-1}
33 (Paku, 2001). SWAT has no capability to dynamically adjust the groundwater
34 concentration during a simulation run. Therefore we added 0.44 mg N L^{-1} to all

1 model simulations of TN concentration assuming that groundwater concentrations
2 had equilibrated with the applied wastewater nitrogen.

3 **2.3 Model calibration and validation**

4 Daily mean discharge was firstly calibrated based on daily mean values of 15–
5 minute measurements. Water quality variables were then calibrated in the
6 sequence: SS, TP and TN. Modelled mean daily concentrations were compared
7 with concentrations measured during monthly grab sampling, with monthly
8 measurements assumed equal to daily mean concentrations. One year (1993) was
9 used for model warmup. The calibration period was from 2004 to 2008 and the
10 validation period was from 1994 to 1997. A validation period that pre-dated the
11 calibration period was chosen because discharge records were available for two
12 separate periods (1994–1997 and post 2004). In addition, the operational regime
13 for the wastewater irrigation has varied since operations began in 1991, with a
14 marked change occurring in 2002 when operations switched from applying the
15 wastewater load to two blocks (rotated daily for a total of 14 blocks in a week; i.e.,
16 each block irrigated weekly), to 10–14 blocks each irrigated daily. This
17 operational regime continues today and we therefore decided to assign the most
18 recent (post 2002) period (2004–2008) to calibration to ensure that the model was
19 configured to reflect current operations.

20 Parameter values that were not derived from measurements or the
21 literature were assigned based on either automated or manual calibration (Table 3).
22 Manual calibration was undertaken for 11 parameters related to TP, while a
23 Sequential Uncertainty Fitting (SUFI-2) procedure was applied to auto-calibrate
24 21 parameters for discharge simulations, nine parameters for SS simulations, and
25 17 parameters related to TN. The SUFI-2 procedure has been integrated into the
26 SWAT Calibration and Uncertainty Program (SWAT-CUP). SUFI-2 is a
27 procedure that efficiently quantifies and constrains parameter uncertainties/ranges
28 from default ranges with the fewest number of iterations (Abbaspour et al., 2004),
29 and has been shown to provide optimal results relative to the use of alternative
30 algorithms (Wu and Chen, 2015). SUFI-2 involves Latin hypercube sampling
31 (LHS), which is a method that generates a sample of plausible parameter values
32 from a multidimensional distribution and ensures that samples cover the entire

1 parameter space, therefore ensuring that the optimum solution is not a local
2 minimum (Marino et al., 2008).

3 The SUFI-2 procedure analyses relative sensitivities of parameters by
4 randomly generating combinations of values for model parameters (Abbaspour et
5 al., 2014). A sample size of 1000 was chosen for each iteration of LHS, resulting
6 in 1000 combinations of parameters and 1000 simulations. Model performance
7 was quantified for each simulation based on the Nash–Sutcliffe efficiency (*NSE*).
8 An objective function was defined as a linear regression of a combination of
9 parameter values generated by each LHS against the *NSE* value calculated from
10 each simulation. Each compartment was not given weight to formulate the
11 objective function because only one variable was specifically focused on at each
12 time. A parameter sensitivity matrix was then computed based on the changes in
13 the objective function after 1000 simulations. Parameter sensitivity was quantified
14 based on the *p* value from a Student’s t-test, which was used to compare the mean
15 of simulated values with the mean value of measurements (Rice, 2006). A
16 parameter was deemed sensitive by if $p \leq 0.05$ after 1000 simulations (one
17 iteration). Numerous iterations of LHS were conducted. Values of *p* from
18 numerous iterations were averaged for each parameter, and the frequency of
19 iterations where a parameter was deemed sensitive was summed. Rankings of
20 relative sensitivities of parameters were developed based on how frequently the
21 sensitive parameter was identified and the averaged value of *p* calculated from
22 several iterations. The most sensitive parameter was determined based on the
23 frequency that the parameter was deemed sensitive, and the smallest average *p*–
24 value from all iterations.

25 SUFI-2 considers two criteria to constrain uncertainty in each iteration.
26 One is the P-factor, the percentage of measured data bracketed by 95% prediction
27 uncertainty (95PPU). Another is the R-factor, the average thickness of the 95PPU
28 band divided by the standard deviation of measured data. A range was first
29 defined for each parameter based on a synthesis of ranges from similar studies or
30 from the SWAT default range. Parameter ranges were updated after each iteration
31 based on the computation of upper and lower 95% confidence limits. The 95%
32 confidence interval and the standard deviation of a parameter value were derived
33 from the diagonal elements of the covariance matrix, which was calculated from

1 the sensitivity matrix and the variance of the objective function. Steps and
2 equations used in the SUFI-2 procedure to constrain parameter ranges are
3 outlined by Abbaspour et al. (2004).

4 The total numbers of iterations performed for each simulated variable (Q,
5 SS, MINP, ORGN, NH₄-N and NO₃-N) reflected the numbers required to ensure
6 that > 90% of measured data were bracketed by simulated output and the R-factor
7 was close to one. The ‘optimal’ parameter value was obtained when the Nash–
8 Sutcliffe efficiency (NSE) criterion was satisfied (NSE > 0.5; Moriasi et al., 2007).
9 Auto-calibrated parameters for simulations of Q, SS, and TN were changed by
10 absolute values within the given ranges. Some of those given ranges were
11 restricted based on the optimum values calibrated in similar studies. Parameter
12 values for TP simulations were manually-calibrated based on the relative percent
13 deviation from the predetermined values of those auto-calibrated parameters for
14 MINP simulations, given by the objective functions (e.g., NSE). Parameters
15 related to the physical characteristics of the catchment were not changed because
16 their values were considered to be representative of the catchment characteristics.

17 In addition, high-frequency (1–2 h) water quality sampling was
18 undertaken at the FRI stream-gauge during 2010–2012 to derive estimates of
19 daily mean contaminant loads during storm events. Samples were analysed for SS
20 (nine events), TP and TN (both 14 events) over sampling periods of 24–73 h. The
21 sampling programme was designed to encompass pre-event base flow, storm
22 generated quick flow and post-event base flow (Abell et al., 2013). These data
23 permitted calculation of daily discharge-weighted (Q-weighted) mean
24 concentrations to compare with modelled daily mean estimates. We did not use
25 the high-frequency observations to calibrate the model, because of the limited
26 number of high-frequency (1–2 h) samples (nine events for SS and 14 events for
27 TP and TN in 2010–2012). The use of the high-frequency observations for model
28 validation allowed to examine how the model performed during short (1–3 day)
29 high flow periods. The Q-weighted mean concentrations C_{QWM} were calculated as:

30
$$C_{QWM} = \frac{\sum_{i=1}^n C_i Q_i}{\sum_{i=1}^n Q_i} \quad (1)$$

31 where n is number of samples, C_i is contaminant concentration measured at time i,
32 and Q_i is discharge measured at time i.

2.4 Hydrograph and contaminant load separation

The Web-based Hydrograph Analysis Tool (Lim et al., 2005) was applied to partition both measured and simulated discharges into base flow (Q_b) and quick flow (Q_q). An Eckhardt filter parameter of 0.98 and ratio of base flow to total discharge of 0.8 were assumed (cf. Lim et al., 2005). There were a total of 60 days without quick flow during the calibration period (2004–2008) and 1379 days for which hydrograph separation defined both base flow and quick flow.

Contaminant (SS, TP and TN) concentrations (C_{sep}) were partitioned into base flow (C'_b) and quick flow components (C'_q ; cf. Rimmer and Hartmann, 2014) to separately examine the sensitivity of water quality parameters during base flow and quick flow:

$$C_{sep} = \frac{Q_q \times C'_q + Q_b \times C'_b}{Q_q + Q_b} \quad (2)$$

C'_b for each contaminant was estimated as the average concentration for the 60 days with no quick flow. C'_q for each contaminant was calculated by rearranging Eq. (2).

To ensure that C'_q is positive, C'_b is constrained to be the minimum of $\overline{C_{sep}}$ and C_{sep} . Measured and simulated base flow and quick flow contaminant loads were then calculated.

A one-at-a-time (OAT) routine proposed by Morris (1991) was applied to investigate how parameter sensitivity varied between the two flow regimes (base flow and quick flow), based on the ranking of relative sensitivities of parameters that were identified by randomly generating combinations of values for model parameters for each individual variable using the SUFI-2 procedure. OAT sensitivity analysis was then employed by varying the parameter of interest among ten equidistant values within the default range. The natural logarithm was used by Krause et al. (2005) and therefore the standard deviation (STD) of the ln-transformed NSE were used to indicate parameter sensitivity for the two flow regimes.

Parameters were ranked from most to least sensitive on the basis of the sensitivity metric (STD of ln-transformed NSE), using a value of 0.2 as a threshold above which parameters were deemed particularly 'sensitive'. The

threshold value of “0.2” was chosen in this study, based on the median value derived from the calculations of the *STD* of *ln*-transformed NSE. Methods used to separate the two flow constituents and to quantify parameter sensitivity are illustrated in Fig. 2.

2.5 Model evaluation

Model goodness-of-fit was assessed graphically and quantified using coefficient of determination (R^2), Nash–Sutcliffe efficiency (NSE) and percent bias (PBIAS; Table 4). R^2 (range 0 to 1) and NSE (range $-\infty$ to 1) values are commonly used to evaluate SWAT model performance at daily time step (Gassman et al., 2007). PBIAS value indicates the average tendency of simulated outputs to be larger or smaller than observations (Gupta et al., 1999).

Model uncertainty was evaluated by two criteria; R-factor and P-factor (see Section 2.3). They were used to constrain parameter ranges during the calibration using measured Q and loads of SS, MINP, ORGN, $\text{NH}_4\text{-N}$ and $\text{NO}_3\text{-N}$ in the SUFI-2 procedure. The R software was used to graphically show the 95% confidence and prediction intervals for measurement data (Neyman, 1937) and model prediction intervals (Seymour, 1993) for Q and concentrations of SS, TP and TN during the calibration period (2004–2008).

3 Results

3.1 Model performance and uncertainty

Numerous rounds (each comprising 1000 iterations) of LHS were conducted for each simulated variable until the performance criteria were satisfied. The total number of rounds of LHS for each simulated variable was as follows (number in parentheses): Q (7), SS (7), MINP (11), ORGN (10), $\text{NH}_4\text{-N}$ (4) and $\text{NO}_3\text{-N}$ (4). The parameters that provided the best statistical outcomes (i.e, best match to observed data) are given in Table 3. Two criteria (R-factor and P-factor) were used to show model uncertainties for simulations of discharge and contaminant loads, with values as follows: Q (0.97, 0.43), SS (0.48, 0.19), MINP (2.64, 0.14), ORGN (0.47, 0.17), $\text{NH}_4\text{-N}$ (1.16, 0.56) and $\text{NO}_3\text{-N}$ (1.2, 0.29). Model uncertainties for simulations of Q and SS, TP and TN concentrations are shown in Fig. 6.

1 Modelled and measured base flow showed high correspondence, although
2 measured daily mean discharge during storm peaks was often underestimated (Fig.
3 3a and 3e). Annual mean percentages of lateral flow recharge, shallow aquifer
4 recharge and deep aquifer recharge to total water yield were predicted by SWAT
5 as 30%, 10%, 58%, respectively. Modelled SS concentrations overestimated
6 measurements of monthly grab samples by an average of 18.3% during calibration
7 and 0.32% during validation (Fig. 3b and 3f). Measured TP concentrations in
8 monthly grab samples were underestimated by 23.8% during calibration (Fig. 3c)
9 and 24.5% during validation (Fig. 3g). Similarly, measured TP loads were
10 underestimated by 34.5% and 38.4%, during calibration and validation,
11 respectively. Modelled and measured TN concentrations were generally better
12 aligned during base flow (Fig. 3d), apart from a mismatch prior to 1996 when
13 monthly measured TN concentrations were substantially lower than model
14 predictions, although the concentrations gradually increased (Fig. 3h) during the
15 validation period (1994–1997). The average measured TN load increased from
16 134 kg N d⁻¹ prior to 1996, to 190 kg N d⁻¹ post 1996. The comparable increase in
17 modelled TN load was 167 kg N d⁻¹ to 205 kg N d⁻¹, respectively.

18 Statistical evaluations of goodness-of-fit are shown in Table 5. The R²
19 values for discharge were 0.77 for calibration and 0.68 for validation,
20 corresponding to model performance ratings (cf. Moriasi et al., 2007) of ‘very
21 good’ and ‘good’ (Table 4). Similarly, the NSE values for discharge were 0.73
22 (good) for calibration and 0.62 (satisfactory) for validation. Positive PBIAS (7.8%
23 for calibration and 8.8% for validation) indicated a tendency for underestimation
24 of daily mean discharge, however, the low magnitude of PBIAS values
25 corresponded to a performance rating of ‘very good’. The R² values for SS were
26 0.42 (unsatisfactory) for calibration and 0.80 for validation (very good). Similarly,
27 the NSE values for SS were -0.08 (unsatisfactory) for calibration and 0.76 (very
28 good) for validation. The model did not simulate trends well for monthly
29 measured TP and TN concentrations. The R² values for TP and TN were both <
30 0.1 (unsatisfactory) during calibration and validation and NSE values were both <
31 0 (unsatisfactory). Values of PBIAS corresponded to ‘good’ or ‘very good’
32 performance ratings for TP and TN.

1 Observed Q-weighted daily mean concentrations derived from hourly
2 measurements and simulated daily mean concentrations of SS, TP and TN during
3 an example two-day storm event are shown in Fig. 4a–4c. The simulation of SS
4 and TN concentrations was somewhat better than for TP. Comparisons of Q-
5 weighted daily mean concentrations (C_{QWM}) during storm events from 2010 to
6 2012 are shown in Fig. 4d–4f for SS (nine events), TP and TN (both 14 events).
7 The C_{QWM} of TP exceeded the simulated daily mean by between 0.02 and 0.2 mg
8 $P L^{-1}$, and on average, the model underestimated measurements by 69.4% (Fig. 4e).
9 Although R^2 and NSE values for C_{QWM} of TN were unsatisfactory (Table 5), they
10 were both close to the threshold for satisfactory performance (0.5). For C_{QWM} of
11 SS and TP, R^2 and NSE values indicated that the model performance was
12 unsatisfactory. The PBIAS value of -0.87 for C_{QWM} of TN corresponded to model
13 performance ratings of ‘very good’, while the PBIAS values for C_{QWM} of SS and
14 TP were 43.9 and 69.4, respectively, indicating satisfactory model performance.

15 Measured and simulated discharge and contaminant loads separated for the
16 two flow regimes (base flow and quick flow) are shown in Fig. 5. Model
17 performance statistics differed between the two flow regimes (Table 6).
18 Simulations of discharge and constituent loads under quick flow were more
19 closely related to the measurements (i.e., higher values of R^2 and NSE) than
20 simulations under base flow. Base flow TN load simulations during the validation
21 period showed better model performance than simulations under quick flow.
22 Additionally, measurements under quick flow were better reproduced by the
23 model than the measurements for the whole simulation period. Simulations of
24 contaminant loads matched measurements much better than for contaminant
25 concentrations, as indicated by statistical values for model performance given in
26 Table 5 and 6.

27 **3.2 Separated parameter sensitivity**

28 Based on the ranking of relative sensitivities of hydrological and water quality
29 parameters derived from the SUFI-2 procedure (see Table 7), the OAT sensitivity
30 analysis undertaken separately for base flow and quick flow identified three
31 parameters that most influenced the quick flow estimates, and five parameters that
32 most influenced the base flow estimates (parameters above the dashed line in Fig.
33 7a). Channel hydraulic conductivity (CH_K2) is used to estimate the peak runoff

1 rate (Lane, 1983). Lateral flow slope length (SLSOIL) and lateral flow travel time
2 (LAT_TIME) have an important controlling effect on the amount of lateral flow
3 entering the stream reach during quick flow. Both slope (HRU_SLP) and soil
4 available water content (SOL_AWC) were particularly sensitive for the base flow
5 simulation because they affect lateral flow within the kinematic storage model in
6 SWAT (Sloan and Moore, 1984). The aquifer percolation coefficient
7 (RCHRG_DP) and the base flow alpha factor (ALPHA_BF) strongly influenced
8 base flow calculations (Sangrey et al., 1984), as did the channel Manning's N
9 value (CH_N2) which is used to estimate channel flow (Chow, 2008).

10 For SS loads, 12 and four parameters, respectively, were identified as
11 sensitive in relation to the simulations of base flow and quick flow (parameters
12 above the dashed line in Fig. 7b). Parameters that control main channel processes
13 (e.g. CH_K2 and CH_N2) and subsurface water transport processes (e.g.
14 LAT_TIME and SLSOIL) were found to be much more sensitive for base flow SS
15 load estimations. Exclusive parameters for SS estimations, such as SPCON (linear
16 parameter), PRF (peak rate adjustment factor), SPEXP (exponent parameter),
17 CH_COV1 (channel erodibility factor), and CH_COV2 (channel cover factor)
18 were found to be much more sensitive in base flow SS load, while LAT_SED (SS
19 concentration in lateral flow and groundwater flow) was more sensitive in quick
20 flow SS load. Parameters that control overland processes, e.g. CN2 (the curve
21 number), OV_N (overland flow Manning's N value) and SLSUBBSN (sub-basin
22 slope length), were found to be much more sensitive for quick flow SS load
23 estimations.

24 Of the sensitive parameters, BC4 (ORGP mineralization rate) was
25 particularly sensitive for the simulation of base flow MINP load (Fig. 7c). RCN
26 (nitrogen concentration in rainfall) related specifically to the dynamics of the base
27 flow NO₃-N load and NPERCO (nitrogen percolation coefficient) significantly
28 affected quick flow NO₃-N load (Fig. 7d). Parameter CH_ONCO (channel ORGN
29 concentration) similarly affected both flow components of ORGN load (Fig. 7e)
30 and SOL_CBN (organic carbon content) was most sensitive for the simulations of
31 quick flow ORGN and NH₄-N loads. Parameter BC1 (nitrification rate in reach)
32 was particularly sensitive for the simulation of base flow NH₄-N load (Fig. 7f).

33

4 Discussion

This study examined temporal dynamics of model performance and parameter sensitivity in a SWAT model application that was configured for a small, relatively steep and lower order stream catchment in New Zealand. This country faces increasing pressures on freshwater resources (Parliamentary Commissioner for the Environment, 2013) and models such as SWAT potentially offer valuable tools to inform management of water resources although, to date, the SWAT model has received limited consideration in New Zealand (Cao et al., 2006). Model evaluation on the basis of the data collected during an extended monitoring programme enabled a detailed examination of how model performance varied during different flow regimes. It also permitted error in daily mean estimates of contaminant loads to be quantified with relative precision, allowing assessment of the ability of SWAT model to simulate contaminant loads during storm events when lower-order streams typically exhibit considerable sub-daily variability in both discharge and contaminant concentrations (Zhang et al., 2010). Separating discharge and loads of sediments and nutrients into those associated with base flow and quick flow for separate OAT sensitivity analyses provided important insights into the varying dependency of parameter sensitivity on hydrologic conditions.

4.1 Temporal dynamics of model performance

The modelled estimates of deep aquifer recharge (58%) and combined lateral flow and shallow aquifer recharge (40%) were comparable with estimates derived by Rutherford et al. (2011), who used an alternative catchment model to derive respective estimates of 30% and 70% for these two fluxes. Our decision to deliberately select a validation period (1994–1997) during which the boundary conditions of the system (specifically anthropogenic nutrient loading) differed considerably from the calibration period allowed us to rigorously assess the capability of SWAT to accurately predict water quality under an altered management scenario (i.e. the purpose of most SWAT applications).

Overestimation of TN concentrations prior to 1996 reflects higher $\text{NO}_3\text{-N}$ concentrations in groundwater during the calibration period (2004–2008) due to the wastewater irrigation operation. Nitrate concentrations appeared to reach a new quasi-steady state as wastewater loads and in-stream attenuation came into

1 balance. SWAT may not adequately represent the dynamics of groundwater
2 nutrient concentrations (Bain et al., 2012) particularly in the presence of changes
3 in catchment inputs (e.g., with start-up of wastewater irrigation). The
4 groundwater delay parameter was set to five years (cf. Rotorua District Council,
5 2006), but this did not appear to capture adequately the lag in response to
6 increases in stream nitrate concentrations following wastewater irrigation from
7 1991.

8 The poor fit between simulated daily mean TP concentrations and monthly
9 instantaneous measurements may partly reflect a mismatch between the dominant
10 processes affecting phosphorus cycling in the stream and those represented in
11 SWAT. The ORGP fraction that is simulated in SWAT includes both organic and
12 inorganic forms of particulate phosphorus, however, the representation of
13 particulate phosphorus cycling only focusses on organic phosphorus cycling, with
14 limited consideration of interactions between inorganic streambed sediments and
15 dissolved reactive phosphorus in the overlying water (White et al., 2014). This
16 contrasts with phosphorus cycling in the study stream where it has been shown
17 that dynamic sorption processes between the dissolved and particulate inorganic
18 phosphorus pools exert major control on phosphorus cycling (Abell and Hamilton,
19 2013).

20 Our finding that measured Q-weighted mean concentrations (C_{QWM}) of TP
21 and SS during storm events (2010–2012) were greatly underestimated relative to
22 simulated daily mean TP and SS concentrations has important implications for
23 studies that examine effects of altered flow regimes on contaminant transport. For
24 example, studies which simulate scenarios comprising more frequent large rainfall
25 events (associated with climate change predictions for many regions; IPCC, 2013)
26 may considerably underestimate projected future loads of SS and associated
27 particulate nutrients if only base flow water quality measurements (i.e. those
28 predominantly collected during ‘state of environment’ monitoring) are used for
29 calibration/validation (see Radcliffe et al., 2009 for a discussion of this issue in
30 relation to phosphorus). This is also reflected by the two model performance
31 statistics relating to validation of modelled SS concentrations using monthly grab
32 samples (predominantly base flow; ‘very good’) and C_{QWM} estimated during
33 storm sampling (‘unsatisfactory’) based on R^2 and NSE values.

1 **4.2 Key uncertainties**

2 Model uncertainty in this study may arise from four main factors: 1) model
3 parameters; 2) forcing data; 3) in measurements used for evaluation of model fit,
4 and; 4) model structure or algorithms (Lindenschmidt et al., 2007). The values of
5 most parameters assigned for model calibration, although specific to different soil
6 types (e.g. soil parameters), were lumped across land uses and slopes in this study.
7 They integrated spatial and temporal variations, thus neglecting any variability
8 throughout the study catchment. In terms of forcing data, the assumption of
9 constant values of spring discharge rate and nutrient concentrations may
10 inadequately reflect the temporal variability and therefore increase model
11 uncertainty, although this should contribute little to the model error term. Most
12 water quality data used for model calibration comprised monthly instantaneous
13 samples taken during base flow conditions. The use of those measurements for
14 model calibration would likely lead to considerable underestimation of constituent
15 concentrations (notably SS and TP) due to failure to account for short-term high
16 flow events. Inadequate representation of groundwater processes in the model
17 structure is another key factor that is likely to affect model uncertainty,
18 particularly for nitrogen simulations. The analysis of model performance based on
19 datasets separated into base flow and quick flow constituents enabled
20 uncertainties in the structure of hydrological models to be identified, denoted by
21 different model performance between these two flow constituents. Furthermore,
22 the disparity in goodness-of-fit statistics between discharge (typically ‘good’ or
23 ‘very good’) and nutrient variables (often ‘unsatisfactory’) highlights the potential
24 for catchment models which inadequately represent contaminant cycling
25 processes (manifest in unsatisfactory concentration estimates) to nevertheless
26 produce satisfactorily load predictions (e.g., compare model performance statistics
27 for prediction of nutrient concentrations in Table 5 with statistics for prediction of
28 loads in Table 6). This highlights the potential for model uncertainty to be
29 underestimated in studies which aim to predict the effects of scenarios associated
30 with changes in contaminant cycling, such as increases in fertiliser application
31 rates.

4.3 Temporal dynamics of parameter sensitivity

To date, studies of temporal variability of parameters have focused on hydrological parameters, rather than on water quality parameters. The characteristics of concentration–discharge relationships for SS and TP are different to that for TN (Abell et al., 2013). In quick flow, there is a positive relationship between Q and concentrations of SS and TP, reflecting mobilisation of sediments and associated particulate P. Total nitrogen concentrations declined slightly in quick flow, reflecting the dilution of nitrate from groundwater. Defining separate contaminant concentrations in base flow and quick flow enabled us to examine how the sensitivity of water quality parameters varied depending on hydrologic conditions.

In a study of a lowland catchment (481 km²), Guse et al. (2014) found that three groundwater parameters, RCHRG_DP (aquifer percolation coefficient), GW_DELAY (groundwater delay) and ALPHA_BF (base flow alpha factor) were highly sensitive in relation to simulating discharge during quick flow, while ESCO (soil evaporation compensation factor) was most sensitive during base flow. This is counter to the findings of this study for which the base–flow discharge simulation was sensitive to RCHRG_DP and ALPHA_BF. This result may reflect that, relative to our study catchment, the catchment studied by Guse et al. (2014) had moderate precipitation (884 mm y⁻¹) with less forest cover and flatter topography. Although the GW_DELAY parameter reflects the time lag that it takes water in the soil water to enter the shallow aquifers, its lack of sensitivity under both base flow and quick flow conditions in this study is a reflection of higher water infiltration rates and steeper slopes. The ESCO parameter controls the upwards movement of water from lower soil layers to meet evaporative demand (Neitsch et al., 2011). Its lack of sensitivity in our study may reflect relatively high and seasonally–consistent rainfall (1500 mm y⁻¹), in addition to extensive forest cover in the Puarenga Stream catchment, which reduces soil evaporative demand by shading. Soil texture is also likely a contributor to this result. The predominant soil horizon type in the Puarenga Stream catchment was A, indicating high macroporosity which promotes high water infiltration rate and inhibits upward transport of water by capillary action (Neitsch et al., 2011). The variability in the sensitivity of the parameter SURLAG (surface runoff lag coefficient) between this study (relatively insensitive) and that of Cibin et al.

1 (2010; relatively sensitive) likely reflects differences in catchment size. The
2 Puarenga Stream catchment (77 km²) is much smaller than the study catchment
3 (St Joseph River; 2800 km²) of Cibin et al. (2010) and, consequently, distances to
4 the main channel are much shorter, with less potential for attenuation of surface
5 runoff in off-channel storage sites. The curve number (CN2) parameter was found
6 to be insensitive in both this study and Shen et al. (2012), because surface runoff
7 was simulated based on the Green and Ampt method (1911) requiring the hourly
8 rainfall inputs, rather than the curve number equation which is an empirical model.
9 By contrast, the most sensitive parameters in our study are those that determine
10 the extent of lateral flow, an important contributor to streamflow in the catchment,
11 due to a general lack of ground cover under plantation trees and formation of
12 gully networks on steep terrain.

13 Parameters that control surface water transport processes (e.g. LAT_TIME
14 and SLSOIL) were found to be much more sensitive for base flow SS load
15 estimation than parameters that control groundwater processes (e.g. ALPHA_BF
16 and RCHRG_DP), reflecting the importance of surface flow processes for
17 sediment transport. Sensitive parameters for quick flow SS load estimation related
18 to overland flow processes (e.g. OV_N and SLSUBBSN), thus reflecting the fact
19 that sediment transport is largely dependent on rainfall-driven processes, as is
20 typical of steep and lower-order catchments. Modelled base flow NO₃-N loads
21 were most sensitive to the nitrogen concentration in rainfall (RCN) because of
22 rainfall as a predominant contributor to recharging base flow. The nitrogen
23 percolation coefficient (NPERCO) was more influential for quick flow NO₃-N
24 load estimation, probably indicating that the quick flow NO₃-N load is more
25 influenced by the mobilisation of concentrated nitrogen sources associated with
26 agriculture or treated wastewater distribution. High sensitivity of the organic
27 carbon content (SOL_CBN) for quick flow ORGN load estimates likely reflects
28 mobilisation of N associated with organic material following rainfall. The finding
29 that base flow NH₄-N load was more sensitive to nitrification rate in reach (BC1)
30 likely reflects that base flow provides more favourable conditions to complete this
31 oxidation reaction, as NH₄-N is less readily leached and transported. Similarly,
32 the ORGP mineralization rate (BC4) strongly influenced base flow MINP load
33 estimation, reflecting that base flow phosphorus transport is relatively more
34 influenced by cycling from channel bed stores, whereas quick flow phosphorus

1 transport predominantly reflects the transport of phosphorus that originated from
2 sources distant from the channel.

3

4 **5 Conclusions**

5 The performance of a SWAT model was quantified for different hydrologic
6 conditions in a small catchment with mixed land use. Discharge-weighted mean
7 concentrations of TP and SS measured during storm events were greatly
8 underestimated by SWAT, highlighting the potential for uncertainty to be greatly
9 underestimated in catchment model applications that are validated using a sample
10 of contaminant load measurements that is over-represented by measurements
11 made during base flow conditions. Accurate simulation of nitrogen concentrations
12 was constrained by the non-steady state of groundwater nitrogen concentrations
13 due to historic variability in anthropogenic nitrogen applications to land. The
14 sensitivity of many parameters varied depending on the relative dominance of
15 base flow and quick flow, while curve number, soil evaporation compensation
16 factor, surface runoff lag coefficient, and groundwater delay were largely
17 invariant to the two flow regimes. Parameters relating to main channel processes
18 were more sensitive when estimating variables (particularly Q and SS) during
19 base flow, while those relating to overland processes were more sensitive for
20 simulating variables associated with quick flow. Temporal dynamics of both
21 parameter sensitivity and model performance due to dependence on hydrologic
22 conditions should be considered in further model applications. Monitoring
23 programmes which collect high-frequency and event-based data have an
24 important role in supporting the robust calibration and validation of SWAT model
25 applications. This study has important implications for modelling studies of
26 similar catchments that exhibit short-term temporal fluctuations in stream flow. In
27 particular these include small catchments with relatively steep terrain and lower
28 order streams with moderate to high rainfall.

29

30 **Acknowledgements**

31 This study was funded by the Bay of Plenty Regional Council and the Ministry of
32 Business, Innovation and Employment (Outcome Based Investment in Lake
33 Biodiversity Restoration UOWX0505). We thank the Bay of Plenty Regional

1 Council (BoPRC), Rotorua District Council (RDC) and Timberlands Limited for
2 assistance with data collection. In particular, we thank Alison Lowe (RDC),
3 Alastair MacCormick (BoPRC), Craig Putt (BoPRC) and Ian Hinton
4 (Timberlands Limited). Theodore Kpodonu (University of Waikato) is thanked for
5 assisting with manuscript preparation.

1 **References**

- 2 Abbaspour, K.C.: Swat–Cup4: SWAT Calibration and Uncertainty Programs
3 Manual Version 4, Department of Systems Analysis, Integrated
4 Assessment and Modelling (SIAM), Eawag, Swiss Federal Institute of
5 Aquatic Science and Technology, Duebendorf, Switzerland, pp 106, 2014.
- 6 Abbaspour, K.C., Johnson, C.A., and van Genuchten, M.T.H.: Estimating
7 uncertain flow and transport parameters using a sequential uncertainty
8 fitting procedure, *Vadose Zone J.*, 3, 1340–1352, doi:
9 10.2136/vzj2004.1340, 2004.
- 10 Abbaspour, K.C., Yang, J., Maximov, I., Siber, R., Bogner, K., Mieleitner, J.,
11 Zobrist, J., and Srinivasan, R.: Modelling hydrology and water quality in
12 the pre–alpine/alpine Thur watershed using SWAT, *J. Hydrol.*, 333, 413–
13 430, doi: 10.1016/j.jhydrol.2006.09.014, 2007.
- 14 Abell, J.M. and Hamilton, D.P.: Bioavailability of phosphorus transported during
15 storm flow to a eutrophic polymictic lake, *New Zeal. J. Mar. Fresh.*, 47,
16 481–489, doi: 10.1080/00288330.2013.792851, 2013.
- 17 Abell, J.M., Hamilton, D.P., and Rutherford, J.C.: Quantifying temporal and
18 spatial variations in sediment, nitrogen and phosphorus transport in stream
19 inflows to a large eutrophic lake, *Environ. Sci.: Processes Impacts*, 15,
20 1137–1152, doi: 10.1039/c3em00083d, 2013.
- 21 Arnold, J.G., Srinivasan, R., Muttiah, R.S., and Williams, J.R.: Large area
22 hydrologic modeling and assessment Part I: Model development, *J. Am.*
23 *Water Resour. As.*, 34, 73–89, doi: 10.1111/j.1752-1688.1998.tb05961.x,
24 1998.
- 25 Bain, D.J., Green, M.B., Campbell, J.L., Chamblee, J.F., Chaoka, S., Fraterrigo,
26 J.M., Kaushal, S.S., Martin, S.L., Jordan, T.E., and Parolari, A.J.: Legacy
27 effects in material flux: structural catchment changes predate long–term
28 studies, *BioScience*, 62, 575–584, doi: 10.1525/bio.2012.62.6.8, 2012.
- 29 Bi, H.Q., Long, Y.S., Turner, J., Lei, Y.C., Snowdon, P., Li, Y., Harper, R.,
30 Zerihun, A., and Ximenes, F.: Additive prediction of aboveground
31 biomass for *Pinus radiata* (D. Don) plantations, *Forest Ecol. Manag.*, 259,
32 2301–2314, doi: 10.1016/j.foreco.2010.03.003, 2010.

1 Bieroza, M.Z., Heathwaite, A.L., Mullinger, N.J., and Keenan, P.O.:
2 Understanding nutrient biogeochemistry in agricultural catchments: the
3 challenge of appropriate monitoring frequencies, *Environ. Sci.: Processes*
4 *Impacts*, 16, 1676–1691, doi: 10.1039/c4em00100a, 2014.

5 Boyle, D.P., Gupta, H.V., and Sorooshian, S.: Toward improved calibration of
6 hydrologic models: Combining the strengths of manual and automatic
7 methods, *Water Resour. Res.*, 36, 3663–3674,
8 doi: 10.1029/2000WR900207, 2000.

9 Brigode, P., Oudin, L., and Perrin, C.: Hydrological model parameter instability:
10 A source of additional uncertainty in estimating the hydrological impacts
11 of climate change?, *J. Hydrol.*, 476, 410–425, doi:
12 10.1016/j.jhydrol.2012.11.012, 2013.

13 Cao, W., Bowden, W.B., Davie, T., and Fenemor, A.: Multi-variable and multi-
14 site calibration and validation of SWAT in a large mountainous catchment
15 with high spatial variability, *Hydrol. Process.*, 20, 1057–1073,
16 doi: 10.1002/hyp.5933, 2006.

17 Chiwa, M., Ide, J., Maruno, R., Higashi, N., and Otsuki, K.: Effects of storm flow
18 samplings on the evaluation of inorganic nitrogen and sulfate budgets in a
19 small forested watershed, *Hydrol. Process.*, 24, 631–640, doi:
20 10.1002/hyp.7557, 2010.

21 Choi, H.T. and Beven, K.J.: Multi-period and multi-criteria model conditioning
22 to reduce prediction uncertainty in an application of TOPMODEL within
23 the GLUE framework, *J. Hydrol. (NZ)*, 332, 316–336, doi:
24 10.1016/j.jhydrol.2006.07.012, 2007.

25 Chow, V.T.: *Open-channel hydraulics*, Blackburn Press, Caldwell, New Jersey,
26 2008.

27 Cibin, R., Sudheer, K.P., and Chaubey, I.: Sensitivity and identifiability of stream
28 flow generation parameters of the SWAT model, *Hydrol. Process.*, 24,
29 1133–1148, doi: 10.1002/hyp.7568, 2010.

30 Conan, C., Bouraoui, F., Turpin, N., de Marsily, G., and Bidglio, G.: Modelling
31 flow and nitrate fate at catchment scale in Brittany (France), *J. Environ.*
32 *Qual.*, 32, 2026–2032, doi:10.2134/jeq2003.2026, 2003. Dairying Research
33 Corporation, AgResearch, Fert Research: Fertilizer use on New Zealand
34 Dairy Farms, In *New Zealand Fertiliser Manufacturers' Research*

1 Association, Roberts, A.H.C. and Morton, J.D. (eds), Auckland, New
2 Zealand, 36, 1999.

3 Eckhardt, K. and Arnold, J.G.: Automatic calibration of a distributed catchment
4 model, *J. Hydrol.*, 251, 103–109, 2001.

5 Ekanayake, J. and Davie, T.: The SWAT model applied to simulating nitrogen
6 fluxes in the Motueka River catchment, Landcare Research ICM Report
7 2004–05/04, Landcare Research, Lincoln, New Zealand, 18, 2005.

8 Environment Bay of Plenty: Historical data summary, Report prepared for Bay of
9 Plenty Regional Council, New Zealand, 522. 2007.

10 Fert Research: Fertilizer Use on New Zealand Sheep and Beef Farms, In New
11 Zealand Fertiliser Manufacturers' Research Association, Balance, J.M.
12 and Ravensdown, A.R. (eds), Newmarket, Auckland, New Zealand, 52,
13 2009.

14 Gassman, P.W., Reyes, M.R., Green, C.H., and Arnold, J.G.: The Soil and Water
15 Assessment Tool: Historical development, applications, and future
16 research directions, *T. ASABE*, 50, 1211–1250, 2007.

17 Glover, R.B.: Rotorua Chemical Monitoring to June 1993, GNS Client Report
18 prepared for Bay of Plenty Regional Council, #722305.14, Bay of Plenty
19 Regional Council, New Zealand, 38, 1993.

20 Green, W.H. and Ampt, G.A.: Studies on soil physics, part I – the flow of air and
21 water through soils, *J. Agr. Sci.*, 4, 1–24, doi:
22 10.1017/S0021859600001441, 1911.

23 Gupta, H.V., Sorooshian, S., and Yapo, P.O.: Status of automatic calibration for
24 hydrologic models: Comparison with multilevel expert calibration, *J.*
25 *Hydrol. Eng.*, 4, 135–143, doi: 10.1061/(ASCE)1084–0699(1999)4:2(135),
26 1999.

27 Guse, B., Reusser, D.E., and Fohrer, N.: How to improve the representation of
28 hydrological processes in SWAT for a lowland catchment–temporal
29 analysis of parameter sensitivity and model performance, *Hydrol. Process.*,
30 28, 2651–2670, doi: 10.1002/hyp.9777, 2014.

31 Hall, G.M.J., Wiser, S.K., Allen, R.B., Beets, P.N., and Goulding, C.J.: Strategies
32 to estimate national forest carbon stocks from inventory data: the 1990
33 New Zealand baseline, *Glob. Change Biol.*, 7, 389–403,
34 doi: 10.1046/j.1365–2486.2001.00419.x, 2001.

1 Hopmans, P. and Elms, S.R.: Changes in total carbon and nutrients in soil profiles
2 and accumulation in biomass after a 30-year rotation of *Pinus radiata* on
3 podzolized sands: Impacts of intensive harvesting on soil resources, *Forest*
4 *Ecol. Manag.*, 258, 2183–2193, doi: 10.1016/j.foreco.2009.02.010, 2009.

5 IPCC: Climate Change 2013: The Physical Science Basis. Contribution of
6 Working Group I to the Fifth Assessment Report of the Intergovernmental
7 Panel on Climate Change. Stocker, T.F., Qin, D., Plattner, G.K., Tignor,
8 M., Allen, S.K., Boschung, J., Nauels, A., Xia, Y., Bex, V., and Midgley,
9 P.M. (eds), Cambridge University Press, Cambridge, United Kingdom and
10 New York, NY, USA, 1535, 2013.

11 Jowett, I.: Instream habitat and minimum flow requirements for the Waipa Stream,
12 Ian Jowett Consulting Client report: IJ0703, Report prepared for Rotorua
13 District Council, Rotorua, New Zealand, 31, 2008.

14 Kirschbaum, M.U.F. and Watt, M.S.: Use of a process-based model to describe
15 spatial variation in *Pinus radiata* productivity in New Zealand, *Forest Ecol.*
16 *Manag.*, 262, 1008–1019, doi: 10.1016/j.foreco.2011.05.036, 2011.

17 Krause, P., Boyle, D.P., and Bäse, F.: Comparison of different efficiency criteria
18 for hydrological model assessment, *Advances in Geosciences*, 5, 89–97,
19 2005.

20 Kusabs, I. and Shaw, W.: An ecological overview of the Puarenga Stream with
21 particular emphasis on cultural values: prepared for Rotorua District
22 Council and Environment Bay of Plenty, Rotorua, New Zealand, 42, 2008.

23 Lane, L.J.: Chapter 19: Transmission Losses, In *Soil Conservation Service*,
24 *National engineering handbook*, section 4: hydrology, U.S. Government
25 Printing Office, Washington, D.C., 19-1–19-21, 1983.

26 Ledgard, S. and Thorrold, B.: Nitrogen Fertilizer Use on Waikato Dairy Farms,
27 AgResearch and Dexcel, New Zealand, 5, 1998.

28 Lim, K.J., Engel, B.A., Tang, Z., Choi, J., Kim, K., Muthukrishnan, S., and
29 Tripathy, D.: Automated Web GIS-based Hydrograph Analysis Tool,
30 WHAT, *J. Am. Water Resour. As.*, 41, 1407–1416, doi: 10.1111/j.1752-
31 1688.2005.tb03808.x, 2005.

32 Lindenschmidt, K., Fleischbein, K., and Baborowski, M.: Structural uncertainty in
33 a river water quality modelling system, *Ecol. Model.*, 204, 289–300,
34 doi: 10.1016/j.ecolmodel.2007.01.004, 2007.

- 1 Lowe, A., Gielen, G., Bainbridge, A., and Jones, K.: The Rotorua Land Treatment
2 Systems after 16 years, In New Zealand Land Treatment Collective–
3 Proceedings for 2007 Annual Conference, Rotorua, 14–16 March 2007,
4 66–73, 2007.
- 5 Mahon, W.A.J.: The Rotorua geothermal field: technical report of the Geothermal
6 Monitoring Programme, 1982–1985, Ministry of Energy, Oil and Gas
7 Division, Wellington, New Zealand, 1985.
- 8 Marino, S., Hogue, I.B., Ray, C.J., and Kirschner, D.E.: A methodology for
9 performing global uncertainty and sensitivity analysis in systems biology,
10 J. Theor. Biol., 254, 178–196, doi: 10.1016/j.jtbi.2008.04.011, 2008.
- 11 McKenzie, B.A., Kemp, P.D., Moot, D.J., Matthew, C., and Lucas, R.J.:
12 Environmental effects on plant growth and development, In New Zealand
13 Pasture and Crop Science, White, J.G.H. and Hodgson, J. (eds), Oxford
14 University Press: Auckland, New Zealand, 29–44, 1999.
- 15 Monteith, J.L.: Evaporation and the environment. In the state and movement of
16 water in living organisms, 19th Symposia of the Society for Experimental
17 Biology, Cambridge Univ. Press, London, U.K., 1965.
- 18 Moriassi, D.N., Arnold, J.G., Van Liew, M.W., Bingner, R.L., Harmel, R.D., and
19 Veith, T.L.: Model evaluation guidelines for systematic quantification of
20 accuracy in watershed simulations, T. ASAE, 50, 885–900, 2007.
- 21 Morris, M.D.: Factorial sampling plans for preliminary computational
22 experiments, Technometrics, 33, 161–174, 1991.
- 23 Neitsch, S.L., Arnold, J.G., Kiniry, J.R., and Williams, J.R.: Soil and Water
24 Assessment Tool Theoretical Documentation Version 2009, Texas Water
25 Resources Institute Technical Report No. 406, Texas A&M University
26 System, College Station, Texas, 647, 2011.
- 27 Neyman, J.: Outline of a Theory of Statistical Estimation Based on the Classical
28 Theory of Probability, Phil. Trans. R. Soc. A, 236, 333–380, doi:
29 10.1098/rsta.1937.0005, 1937.Nielsen, A., Trolle, D., Me, W., Luo, L.C.,
30 Han, B.P., Liu, Z.W., Olesen, J.E., and Jeppesen, E.: Assessing ways to
31 combat eutrophication in a Chinese drinking water reservoir using SWAT,
32 Mar. Freshwater Res., 64, 475–492, doi: 10.1071/MF12106, 2013.
- 33 Paku, L.K.: The use of carbon–13 to trace the migration of treated wastewater and
34 the chemical composition in a forest environment, Master Thesis, Science

1 in Chemistry, the University of Waikato, Hamilton, New Zealand, 92,
2 2001.

3 Parliamentary Commissioner for the Environment: Water Quality in New Zealand:
4 Land Use and Nutrient Pollution, New Zealand, 82, 2013.

5 Pfannerstill, M., Guse, B., and Fohrer, N.: Smart low flow signature metrics for an
6 improved overall performance evaluation of hydrological models, *J.*
7 *Hydrol.*, 510, 447–458, 2014.

8 Radcliffe, D.E., Lin, Z., Risse, L.M., Romeis, J.J., and Jackson, C.R.: Modeling
9 phosphorus in the Lake Allatoona watershed using SWAT: I. Developing
10 phosphorus parameter values, *J. Environ. Qual.*, 38, 111–120,
11 doi:10.2134/jeq2007.0110, 2009.

12 Reusser, D.E., Blume, T., Schaefli, B., and Zehe, E.: Analysing the temporal
13 dynamics of model performance for hydrological models, *Hydrol. Earth.*
14 *Syst. Sc.*, 13, 999–1018, doi:10.5194/hess-13-999-2009, 2009.

15 Reusser, D.E. and Zehe, E.: Inferring model structural deficits by analysing
16 temporal dynamics of model performance and parameter sensitivity, *Water*
17 *Resour. Res.*, 47, W07550, 15pp, doi: 10.1029/2010WR009946, 2011.

18 Rice, J.A.: Mathematical statistics and data analysis, Boston, MA, Cengage
19 Learning, 2006.

20 Rimmer, A. and Hartmann, A.: Optimal hydrograph separation filter to evaluate
21 transport routines of hydrological models, *J. Hydrol.*, 514, 249–257, doi:
22 10.1016/j.jhydrol.2014.04.033, 2014.

23 Rotorua District Council, Rotorua Wastewater Treatment Plant, Rotorua, New
24 Zealand, 22, 2006.

25 Rutherford, K., Palliser, C., Wadhwa, S.: Prediction of nitrogen loads to Lake
26 Rotorua using the ROTAN model, Report prepared for Bay of Plenty
27 Regional Council, New Zealand, 183. 2011.

28 Sangrey, D.A., Harrop–Williams, K.O., and Klaiber, J.A.: Predicting ground–
29 water response to precipitation, *J. Geotech. Eng.*, 110, 957–975, doi:
30 10.1061/(ASCE)0733–9410(1984)110:7(957), 1984.

31 Schuol, J., Abbaspour, K.C., Yang, H., and Srinivasan, R.: Modeling blue and
32 green water availability in Africa, *Water Resour. Res.*, 44, W07406, 18 pp,
33 doi: 10.1029/2007WR006609, 2008.

1 Seymour, G.: Predictive Inference: An Introduction, Chapman & Hall, New York,
2 pp 280, 1993.

3 Shen, Z.Y., Chen, L., and Chen, T.: Analysis of parameter uncertainty in
4 hydrological and sediment modeling using GLUE method: a case study of
5 SWAT model applied to Three Gorges Reservoir Region, China, Hydrol.
6 Earth. Syst. Sc., 16, 121–132, doi: 10.5194/hess-16-121-2012, 2012.

7 Sloan, P.G. and Moore, I.D.: Modelling subsurface stormflow on steeply sloping
8 forested watersheds, Water Resour. Res., 20, 1815–1822,
9 doi: 10.1029/WR020i012p01815, 1984.

10 Statistics New Zealand: Fertiliser use in New Zealand, Statistics New Zealand,
11 New Zealand, 13, 2006.

12 van Griensven, A., Meixner, T., Grunwald, S., Bishop, T., Diluzio, M., and
13 Srinivasan, R.: A global sensitivity analysis tool for the parameters of
14 multi-variable catchment models, J. Hydrol., 324, 10–23, doi:
15 10.1016/j.jhydrol.2005.09.008, 2006.

16 Watt, M.S., Clinton, P.W., Coker, G., Davis, M.R., Simcock, R., Parfitt, R.L., and
17 Dando, J.: Modelling the influence of environment and stand
18 characteristics on basic density and modulus of elasticity for young *Pinus*
19 *radiata* and *Cupressus lusitanica*, Forest Ecol. Manag., 255, 1023–1033,
20 doi: 10.1016/j.foreco.2007.09.086, 2008.

21 White, K.L. and Chaubey, I.: Sensitivity analysis, calibration, and validations for
22 a multisite and multivariable SWAT model, J. Am. Water Resour. As., 41,
23 1077–1089, doi: 10.1111/j.1752-1688.2005.tb03786.x, 2005.

24 White, M.J., Storm, D.E., Mittelstet, A., Busteed, P.R., Haggard, B.E., and Rossi,
25 C.: Development and testing of an in-stream phosphorus cycling model
26 for the Soil and Water Assessment Tool, J. Environ. Qual., 43, 215–223,
27 doi: 10.2134/jeq2011.0348, 2014.

28 White, P.A., Cameron, S.G., Kilgour, G., Mroczek, E., Bignall, G., Daughney, C.,
29 and Reeves, R.R.: Review of groundwater in Lake Rotorua catchment,
30 Prepared for Environment Bay of Plenty, Institute of Geological &
31 Nuclear Sciences Client Report 2004/130, Whakatane, New Zealand, 245,
32 2004.

1 Whitehead, D., Kelliher, F.M., Lane, P.M., and Pollock, D.S.: Seasonal
2 partitioning of evaporation between trees and understorey in a widely
3 spaced *Pinus radiata* stand, J. Appl. Ecol., 31, 528–542, 1994.

4 Wu, H., Chen, B. 2015. Evaluating uncertainty estimates in distributed
5 hydrological modeling for the Wenjing River watershed in China by
6 GLUE, SUFI-2, and ParaSol methods. Ecological Engineering 76: 110–
7 121.

8 Ximenes, F.A., Gardner, W.D., and Kathuria, A.: Proportion of above-ground
9 biomass in commercial logs and residues following the harvest of five
10 commercial forest species in Australia, Forest Ecol. Manag., 256, 335–346,
11 doi: 10.1016/j.foreco.2008.04.037, 2008.

12 Yilmaz, K.K., Gupta, H.V., and Wagener, T.: A process-based diagnostic
13 approach to model evaluation: Application to the NWS distributed
14 hydrologic model, Water Resour. Res., 44, W09417, 18 pp, doi:
15 10.1029/2007WR006716, 2008.

16 Zhang, H., Huang, G.H., Wang, D.L., and Zhang, X.D.: Multi-period calibration
17 of a semi-distributed hydrological model based on hydroclimatic
18 clustering, Adv. Water Resour., 34, 1292–1303, 2011.

19 Zhang, Z., Tao, F., Shi, P., Xu, W., Sun, Y., Fukushima, T., and Onda, Y.:
20 Characterizing the flush of stream chemical runoff from forested
21 watersheds, Hydrol. Process., 24, 2960–2970, doi: 10.1002/hyp.7717,
22 2010.

1 Table 1. Description of data used to configure and calibrate the SWAT model.

| Data | Application | Data description and configuration details | Source |
|--|--|--|--|
| Digital elevation model (DEM) & digitized stream network | Sub-basin delineation (Fig. 1b) | 25 m resolution. Used to define five slope classes: 0–4%, 4–10%, 10–17%, 17–26% and >26%. | Bay of Plenty Regional Council (BoPRC) |
| Stream discharge and water quality measurements | Calibration (2004–2008) and validation ¹ (1994–1997; 2010–2012) | FRI: 15-min stream discharge data were aggregated as daily mean values (1994–1997; 2004–2008), monthly grab samples for determination of suspended sediment (SS), total phosphorus (TP) and total nitrogen (TN) concentrations (1994–1997; 2004–2008), high-frequency event-based samples for concentrations of SS (nine events), TP and TN (both 14 events) at 1–2 h frequency (2010–2012). | BoPRC; Abell et al., 2013 |
| Spring discharge and nutrient loads | Point source (Fig. 1b) | Constant daily discharge and nutrient concentrations assigned to two cold-water springs (Waipa Spring and Hemo Spring) and one geothermal spring. | White et al., 2004; Proffit, 2009 (Unpublished Site Visit Report); Paku, 2001; Mahon, 1985; Glover, 1993; Rotorua District Council (pers. comm.) |
| Water abstraction volumes | Water use | Monthly water abstraction assigned to two cold-water springs. | Kusabs and Shaw, 2008; Jowett, 2008 |
| Land use | HRU definition | 25 m resolution, 10 basic land-cover categories. Some particular land-cover parameters were prior-estimated (Table 2). | New Zealand Land Cover Database Version 2; BoPRC |
| Soil characteristics | HRU definition | 22 soil types. Properties were quantified based on measurements (if available) or estimated using regression | New Zealand Land Resource Inventory & digital soil map |

¹ Model validation was undertaken using two different datasets. The monthly measurements (1994–1997) were predominantly collected when base flow was the dominant contributor to stream discharge. Data from high-frequency sampling during rain events (2010–2012) were also used to validate model performance during periods when quick flow was high.

| | | | |
|--|--|---|--|
| | | analysis to estimate properties for unmeasured functional horizons. | (available at http://smap.landcareresearch.co.nz) |
| Meteorological data | Meteorological forcing | Daily maximum and minimum temperature, daily mean relative humidity, daily global solar radiation, daily (9 am) surface wind speed and hourly precipitation. | Rotorua Airport Automatic Weather Station, National Climate Database (available at http://cliflo.niwa.co.nz/); Kaituna rain gauge (Fig. 1a) |
| Agricultural management practices | Agricultural management schedules | Stock density Applications of urea and di-ammonium phosphate Applications of manure-associated nutrients | Statistics New Zealand, 2006; Ledgard and Thorrold, 1998 Statistics New Zealand, 2006; Fert Research, 2009 Dairying Research Corporation, 1999 |
| Nutrient loading by wastewater application | Nonpoint-source from land treatment irrigation | Wastewater application rates and effluent composition (TN and TP concentration) for 16 spray blocks from 1996–2012. Each spray block was assigned an individual management schedule specifying daily application rates. | Rotorua District Council, 2006 |
| Forest stand map and harvest dates | Forestry planting and harvesting operations | Planting and harvesting data for 472 ha forestry stands. Prior to 2007 we assumed stands were cleared one-year prior to the establishment year. Post 2007, harvesting date was assigned to the first day of harvesting month. | Timberlands Limited, Rotorua, New Zealand (pers. comm.) |

- 1 Table 2. Prior-estimated parameter values for three dominant types of land-cover in the Puarenga Stream catchment. Values of other
- 2 land use parameters were based on the default values in the SWAT database.

| Land-cover type | Parameter | Definition | Value | Source |
|----------------------------------|--|--|----------|----------------------------|
| PINE (<i>Pinus radiata</i>) | HVSTI | Percentage of biomass harvested | 0.65 | (Ximenes et al., 2008) |
| | T_OPT (°C) | Optimal temperature for plant growth | 15 | (Kirschbaum and Watt 2011) |
| | T_BASE (°C) | Minimum temperature for plant growth | 4 | (Kirschbaum and Watt 2011) |
| | MAT_YRS | Number of years to reach full development | 30 | (Kirschbaum and Watt 2011) |
| | BMX_TREES (tonnes ha ⁻¹) | Maximum biomass for a forest | 400 | (Bi et al., 2010) |
| | GSI (m s ⁻¹) | Maximum stomatal conductance | 0.00198 | (Whitehead et al., 1994) |
| | BLAI (m ² m ⁻²) | Maximum leaf area index | 5.2 | (Watt et al., 2008) |
| | BP3 | Proportion of P in biomass at maturity | 0.000163 | (Hopmans and Elms 2009) |
| FRSE (Evergreen forest) | BN3 | Proportion of N in biomass at maturity | 0.00139 | (Hopmans and Elms 2009) |
| | HVSTI | Percentage of biomass harvested | 0 | – |
| | BMX_TREES (tonnes ha ⁻¹) | Maximum biomass for a forest | 372 | (Hall et al., 2001) |
| PAST (Pastoral farm) | MAT_YRS (years) | Number of years for tree to reach full development | 100 | – |
| | T_OPT (°C) | Optimal temperature for plant growth | 25 | (McKenzie et al., 1999) |
| | T_BASE (°C) | Minimum temperature for plant growth | 5 | (McKenzie et al., 1999) |

- 1 Table 3. Summary of calibrated SWAT parameters. Discharge (Q), suspended sediment (SS) and total nitrogen (TN) parameter
- 2 values were assigned using auto-calibration, while total phosphorus (TP) parameters were manually calibrated. SWAT default ranges
- 3 and input file extensions are shown for each parameter.

| Parameter | Definition | Unit | Default range | Calibrated value |
|---------------|---|--------------------------------|---------------|------------------|
| Q | | | | |
| EVRCH.bsn | Reach evaporation adjustment factor | | 0.5–1 | 0.9 |
| SURLAG.bsn | Surface runoff lag coefficient | | 0.05–24 | 15 |
| ALPHA_BF.gw | Base flow alpha factor (0–1) | | 0.0071–0.0161 | 0.01 |
| GW_DELAY.gw | Groundwater delay | d | 0–500 | 500 |
| GW_REVAP.gw | Groundwater “revap” coefficient | | 0.02–0.2 | 0.08 |
| GW_SPYLD.gw | Special yield of the shallow aquifer | m ³ m ⁻³ | 0–0.4 | 0.13 |
| GWHT.gw | Initial groundwater height | m | 0–25 | 14 |
| GWQMN.gw | Threshold depth of water in the shallow aquifer required for return flow to occur | mm | 0–5000 | 372 |
| RCHRG_DP.gw | Deep aquifer percolation fraction | | 0–1 | 0.87 |
| REVAPMN.gw | Threshold depth of water in the shallow aquifer required for “revap” to occur | mm | 0–500 | 260 |
| CANMX.hru | Maximum canopy storage | mm | 0–100 | 0.6 |
| EPCO.hru | Plant uptake compensation factor | | 0–1 | 0.34 |
| ESCO.hru | Soil evaporation compensation factor | | 0–1 | 0.9 |
| HRU_SLP.hru | Average slope steepness | m m ⁻¹ | 0–0.6 | 0.5 |
| LAT_TTIME.hru | Lateral flow travel time | d | 0–180 | 3 |
| RSDIN.hru | Initial residue cover | kg ha ⁻¹ | 0–10000 | 1 |
| SLSOIL.hru | Slope length for lateral subsurface flow | m | 0–150 | 40 |
| CH_K2.rte | Effective hydraulic conductivity in the main channel alluvium | mm h ⁻¹ | 0–500 | 20 |
| CH_N2.rte | Manning's N value for the main channel | | 0–0.3 | 0.16 |

| | | | | |
|--------------|--|------------------------------------|-------------|-------|
| CH_K1.sub | Effective hydraulic conductivity in the tributary channel alluvium | mm h ⁻¹ | 0–300 | 100 |
| CH_N1.sub | Manning's N value for the tributary channel | | 0.01–30 | 20 |
| SS | | | | |
| USLE_P.mgt | USLE equation support practice factor | | 0–1 | 0.5 |
| PRF.bsn | Peak rate adjustment factor for sediment routing in the main channel | | 0–2 | 1.9 |
| SPCON.bsn | Linear parameter for calculating the maximum amount of sediment that can be re-entrained during channel sediment routing | | 0.0001–0.01 | 0.001 |
| SPEXP.bsn | Exponent parameter for calculating sediment re-entrained in channel sediment routing | | 1–1.5 | 1.26 |
| LAT_SED.hru | Sediment concentration in lateral flow and groundwater flow | mg L ⁻¹ | 0–5000 | 5.7 |
| OV_N.hru | Manning's N value for overland flow | | 0.01–30 | 28 |
| SLSUBBSN.hru | Average slope length | m | 10–150 | 92 |
| CH_COV1.rte | Channel erodibility factor | | 0–0.6 | 0.17 |
| CH_COV2.rte | Channel cover factor | | 0–1 | 0.6 |
| TP | | | | |
| P_UPDIS.bsn | Phosphorus uptake distribution parameter | | 0–100 | 0.5 |
| PHOSKD.bsn | Phosphorus soil partitioning coefficient | | 100–200 | 174 |
| PPERCO.bsn | Phosphorus percolation coefficient | | 10–17.5 | 14 |
| PSP.bsn | Phosphorus sorption coefficient | | 0.01–0.7 | 0.5 |
| GWSOLP.gw | Soluble phosphorus concentration in groundwater loading | mg P L ⁻¹ | 0–1000 | 0.063 |
| LAT_ORGP.gw | Organic phosphorus in the base flow | mg P L ⁻¹ | 0–200 | 0.01 |
| ERORGP.hru | Organic phosphorus enrichment ratio | | 0–5 | 2.5 |
| CH_OPCO.rte | Organic phosphorus concentration in the channel | mg P L ⁻¹ | 0–100 | 0.02 |
| BC4.swq | Rate constant for mineralization of organic phosphorus to dissolved phosphorus in the reach at 20 °C | d ⁻¹ | 0.01–0.7 | 0.3 |
| RS2.swq | Benthic (sediment) source rate for dissolved phosphorus in the reach at 20 °C | mg m ⁻² d ⁻¹ | 0.001–0.1 | 0.02 |
| RS5.swq | Organic phosphorus settling rate in the reach at 20 °C | d ⁻¹ | 0.001–0.1 | 0.05 |

| | | | | |
|--------------|---|---------------------------------------|-------------|--------|
| TN | | | | |
| RSDCO.bsn | Residue decomposition coefficient | | 0.02–0.1 | 0.09 |
| CDN.bsn | Denitrification exponential rate coefficient | | 0–3 | 0.3 |
| CMN.bsn | Rate factor for humus mineralization of active organic nitrogen | | 0.001–0.003 | 0.002 |
| N_UPDIS.bsn | Nitrogen uptake distribution parameter | | 0–100 | 0.5 |
| NPERCO.bsn | Nitrogen percolation coefficient | | 0–1 | 0.0003 |
| RCN.bsn | Concentration of nitrogen in rainfall | mg N L ⁻¹ | 0–15 | 0.34 |
| SDNCO.bsn | Denitrification threshold water content | | 0–1 | 0.02 |
| HLIFE_NGW.gw | Half-life of nitrate–nitrogen in the shallow aquifer | d | 0–200 | 195 |
| LAT_ORGN.gw | Organic nitrogen in the base flow | mg N L ⁻¹ | 0–200 | 0.055 |
| SHALLST_N.gw | Nitrate–nitrogen concentration in the shallow aquifer | mg N L ⁻¹ | 0–1000 | 1 |
| ERORGN.hru | Organic nitrogen enrichment ratio | | 0–5 | 3 |
| CH_ONCO.rte | Organic nitrogen concentration in the channel | mg N L ⁻¹ | 0–100 | 0.01 |
| BC1.swq | Rate constant for biological oxidation of ammonium–nitrogen to nitrite–nitrogen in the reach at 20 °C | d ⁻¹ | 0.1–1 | 1 |
| BC2.swq | Rate constant for biological oxidation of nitrite–nitrogen to nitrate–nitrogen in the reach at 20 °C | d ⁻¹ | 0.2–2 | 0.7 |
| BC3.swq | Rate constant for hydrolysis of organic nitrogen to ammonium–nitrogen in the reach at 20 °C | d ⁻¹ | 0.2–0.4 | 0.4 |
| RS3.swq | Benthic (sediment) source rate for ammonium–nitrogen in the reach at 20 °C | mg m ⁻² d ⁻¹ | 0–1 | 0.2 |
| RS4.swq | Rate coefficient for organic nitrogen settling in the reach at 20 °C | d ⁻¹ | 0.001–0.1 | 0.05 |

1 Table 4. Criteria for model performance. Note: o_n is the n^{th} observed datum, s_n is the n^{th} simulated datum, \bar{o} is the observed mean
2 value, \bar{s} is the simulated daily mean value, and N is the total number of observed data. Performance rating criteria are based on
3 Moriasi et al. (2007) for Q: discharge, SS: suspended sediment, TP: total phosphorus and TN: total nitrogen. Moriasi et al. (2007)
4 derived these criteria based on extensive literature review and analysing the reported performance ratings for recommended model
5 evaluation statistics.

| Statistic equation | Constituent | Performance ratings | | | |
|--|-------------|---------------------|--------------|-------------|-----------|
| | | Unsatisfactory | Satisfactory | Good | Very good |
| $R^2 = \frac{\{\sum_{n=1}^N [(s_n - \bar{s})(o_n - \bar{o})]\}^2}{\sum_{n=1}^N (o_n - \bar{o})^2 \times \sum_{n=1}^N (s_n - \bar{s})^2}$ (3) | All | < 0.5 | 0.5 – 0.6 | 0.6 – 0.7 | 0.7 – 1 |
| $NSE = 1 - \frac{\sum_{n=1}^N (o_n - s_n)^i}{\sum_{n=1}^N (o_n - \bar{o})^i}$ $i = 2$ (4) | All | < 0.5 | 0.5 – 0.65 | 0.65 – 0.75 | 0.75 – 1 |
| $\pm \text{PBIAS}\% = \frac{\sum_{n=1}^N (o_n - s_n)}{\sum_{n=1}^N o_n} \times 100$ (5) | Q | > 25 | 15 – 25 | 10 – 15 | < 10 |
| | SS | > 55 | 30 – 55 | 15 – 30 | < 15 |
| | TP, TN | > 70 | 40 – 70 | 25 – 40 | < 25 |

6 R^2 : coefficient of determination

7 NSE: Nash–Sutcliffe efficiency

8 PBIAS: percent bias

- 1 Table 5. Model performance ratings for simulations of discharge (Q), concentrations of suspended sediment (SS), total phosphorus
2 (TP) and total nitrogen (TN). n indicates the number of measurements. Q-weighted mean concentrations were calculated using Eq.
3 (1).

| Model performance | Statistics | Q | SS | TP | TN |
|--|----------------|------------------------|---------------------------|---------------------------|---------------------------|
| | | n = 1439 | n = 43 | n = 45 | n = 39 |
| Calibration with instantaneous measurements (2004–2008) | R ² | 0.77 (Very good) | 0.42 (Unsatisfactory) | 0.02 (Unsatisfactory) | 0.08 (Unsatisfactory) |
| | NSE | 0.73 (Good) | -0.08 (Unsatisfactory) | -1.31 (Unsatisfactory) | -0.30 (Unsatisfactory) |
| | ±PBIAS% | 7.8 (Very good) | -18.3 (Very good) | 23.8 (Very good) | -0.05 (Very good) |
| | | n = 1294 | n = 37 | n = 37 | n = 36 |
| Validation with instantaneous measurements (1994–1997) | R ² | 0.68 (Good) | 0.80 (Very good) | 0.01 (Unsatisfactory) | 0.01 (Unsatisfactory) |
| | NSE | 0.62 (Satisfactory) | 0.76 (Very good) | -0.97 (Unsatisfactory) | -2.67 (Unsatisfactory) |
| | ±PBIAS% | 8.8 (Very good) | -0.32 (Very good) | 24.5 (Very good) | -26.7 (Good) |
| | | – | n = 12 | n = 18 | n = 18 |
| Validation with Q-weighted mean concentrations (2010–2012) | R ² | – | 0.38 (Unsatisfactory) | 0.06 (Unsatisfactory) | 0.46 (Unsatisfactory) |
| | NSE | – | -0.03 (Unsatisfactory) | -4.88 (Unsatisfactory) | 0.42 (Unsatisfactory) |
| | ±PBIAS% | – | 43.9 (Satisfactory) | 69.4 (Satisfactory) | -0.87 (Very good) |

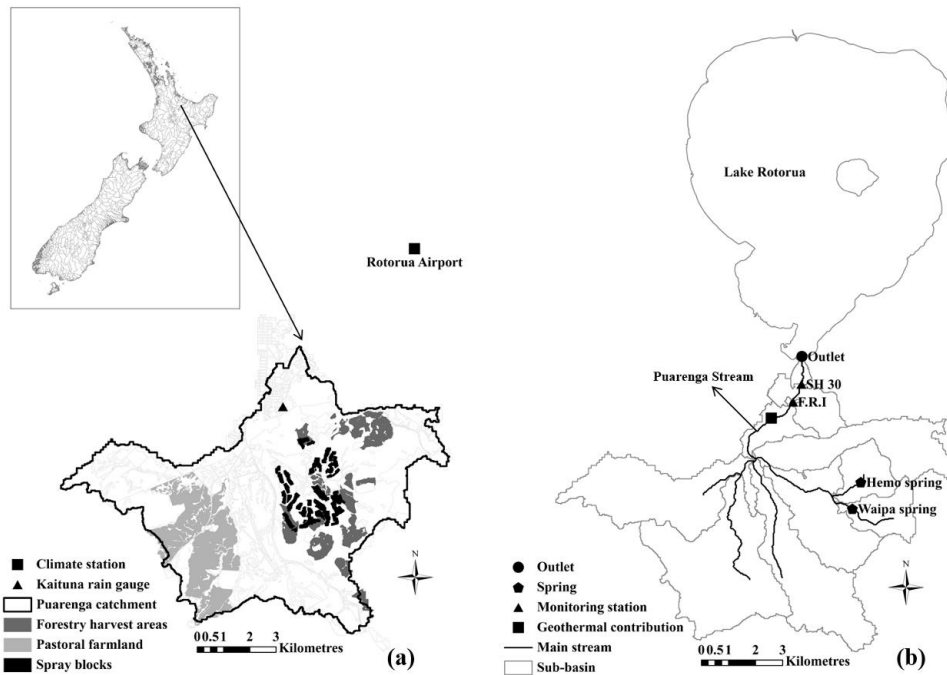
- 1 Table 6. Model performance statistics for simulations of discharge (Q), and loads of suspended sediment (SS), total phosphorus (TP) and total
2 nitrogen (TN). Statistics were calculated for both overall and separated simulations. Q_{all} and L_{all} indicate the overall simulations; Q_b and L_b
3 indicate the base flow simulations; Q_q and L_q indicate the quick flow simulations.

| Model performance | Statistics | Q | | | SS | | | TP | | | TN | | |
|-------------------------|--------------|-------|-------|-----------|-------|-------|-----------|-------|-------|-----------|-------|-------|-----------|
| | | Q_b | Q_q | Q_{all} | L_b | L_q | L_{all} | L_b | L_q | L_{all} | L_b | L_q | L_{all} |
| Calibration (2004–2008) | R^2 | 0.84 | 0.84 | 0.77 | 0.66 | 0.68 | 0.61 | 0.24 | 0.65 | 0.39 | 0.72 | 0.97 | 0.95 |
| | NSE | 0.6 | 0.71 | 0.73 | 0.33 | 0.33 | 0.27 | -6.2 | 0.09 | -0.17 | 0.5 | 0.89 | 0.85 |
| | \pm PBIAS% | 7.5 | 8.7 | 7.8 | 7.57 | -23.4 | -3.6 | 45.4 | 40.1 | 43.6 | 0.8 | 6.6 | 2.7 |
| Validation (1994–1997) | R^2 | 0.87 | 0.81 | 0.68 | 0.36 | 0.98 | 0.95 | 0.27 | 0.27 | 0.06 | 0.79 | 0.33 | 0.58 |
| | NSE | 0.56 | 0.62 | 0.62 | -0.03 | 0.43 | 0.85 | -1.9 | 0.04 | -0.64 | 0.58 | -0.07 | 0.33 |
| | \pm PBIAS% | 11.3 | -1.2 | 8.8 | 34.5 | -79.7 | 11.1 | 45.8 | -9.3 | 37 | -7.6 | 14.3 | -2.5 |

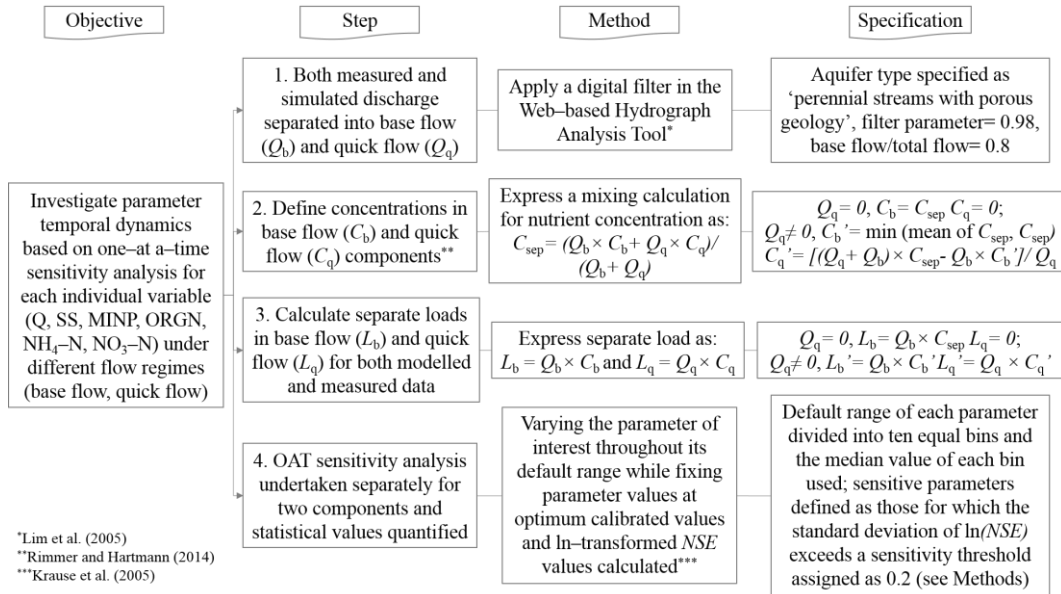
- 4 R^2 : coefficient of determination; NSE: Nash–Sutcliffe efficiency; PBIAS: percent bias

1 Table 7 Rankings of relative sensitivities of parameters (from most to least) for variables (header row) of Q (discharge), SS (suspended sediment),
2 MINP (mineral phosphorus), ORGN (organic nitrogen), NH₄-N (ammonium-nitrogen), and NO₃-N (nitrate-nitrogen). Relative sensitivities
3 were identified by randomly generating combinations of values for model parameters and comparing modelled and measured data with a
4 Student's t test ($p \leq 0.05$). Bold text denotes that a parameter was deemed sensitive relative to more than one simulated variable. Shaded text
5 denotes that parameter deemed insensitive to any of the two flow components (base and quick flow; see Figure 7) using one-at-a-time sensitivity
6 analysis. Definitions and units for each parameter are shown in Table 3.

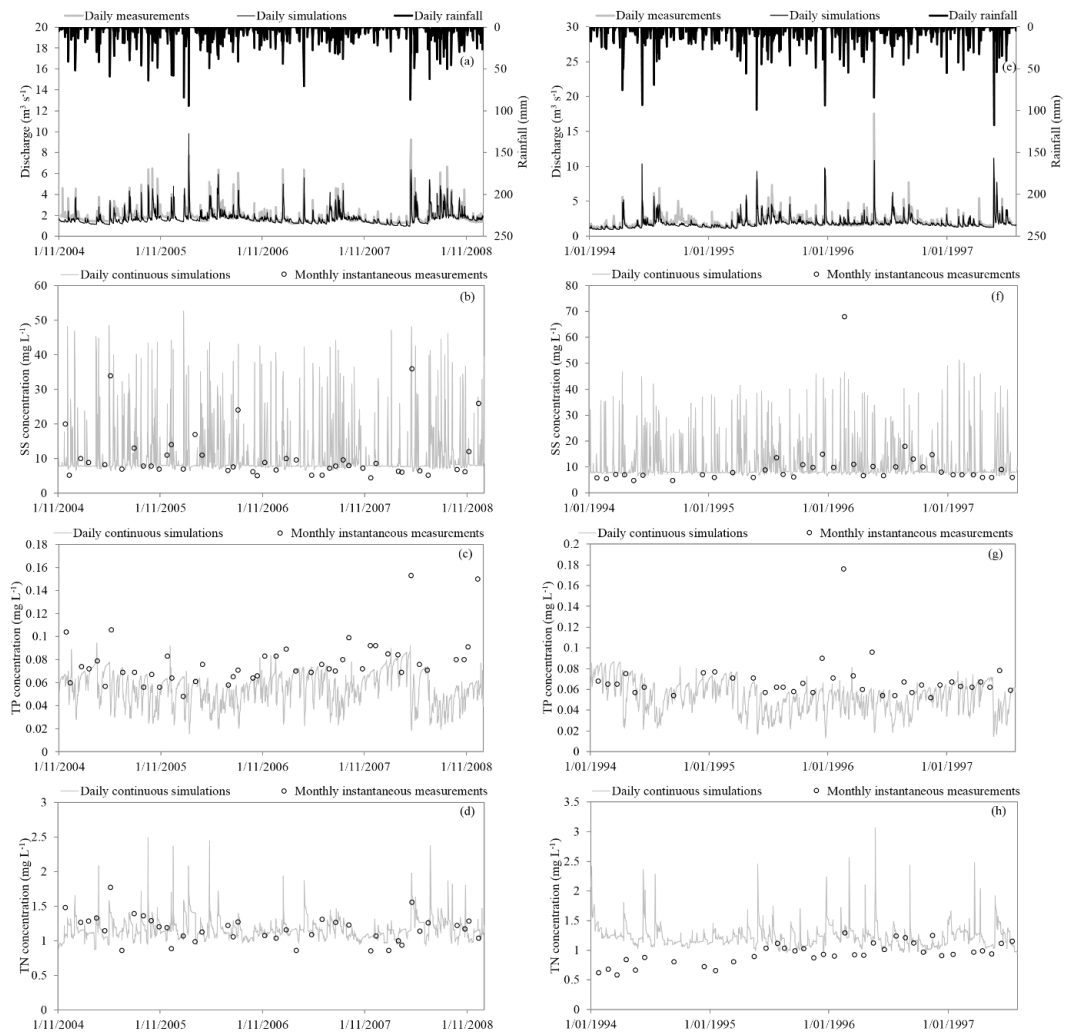
| Q | SS | MINP | ORGN | NH ₄ -N | NO ₃ -N |
|-------------------|-------------------|-----------------|----------------|--------------------|--------------------|
| SLSOIL | LAT_SED | CH_OPCO | CH_ONCO | CH_ONCO | NPERCO |
| CH_K2 | CH_N2 | BC4 | BC3 | BC1 | CDN |
| HRU_SLP | SLSUBBSN | RS5 | SOL_CBN(1) | CDN | ERORGN |
| LAT_TTIME | SPCON | ERORGP | RS4 | RS3 | CMN |
| SOL_AWC(1) | ESCO | PPERCO | RCN | RCN | RCN |
| RCHRG_DP | OV_N | RS2 | N_UPDIS | | RSDCO |
| GWQMN | SLSOIL | PHOSKD | USLE_P | | |
| GW_REVAP | LAT_TTIME | GWSOLP | SDNCO | | |
| GW_DELAY | SOL_AWC(1) | LAT_ORGP | SOL_NO3(1) | | |
| CH_COV1 | EPCO | | CMN | | |
| CH_COV2 | CANMX | | HLIFE_NGW | | |
| EPCO | CH_K2 | | RSDCO | | |
| SPEXP | GW_DELAY | | USLE_K(1) | | |
| CANMX | ALPHA_BF | | | | |
| CH_N1 | GW_REVAP | | | | |
| PRF | CH_COV1 | | | | |
| SURLAG | | | | | |



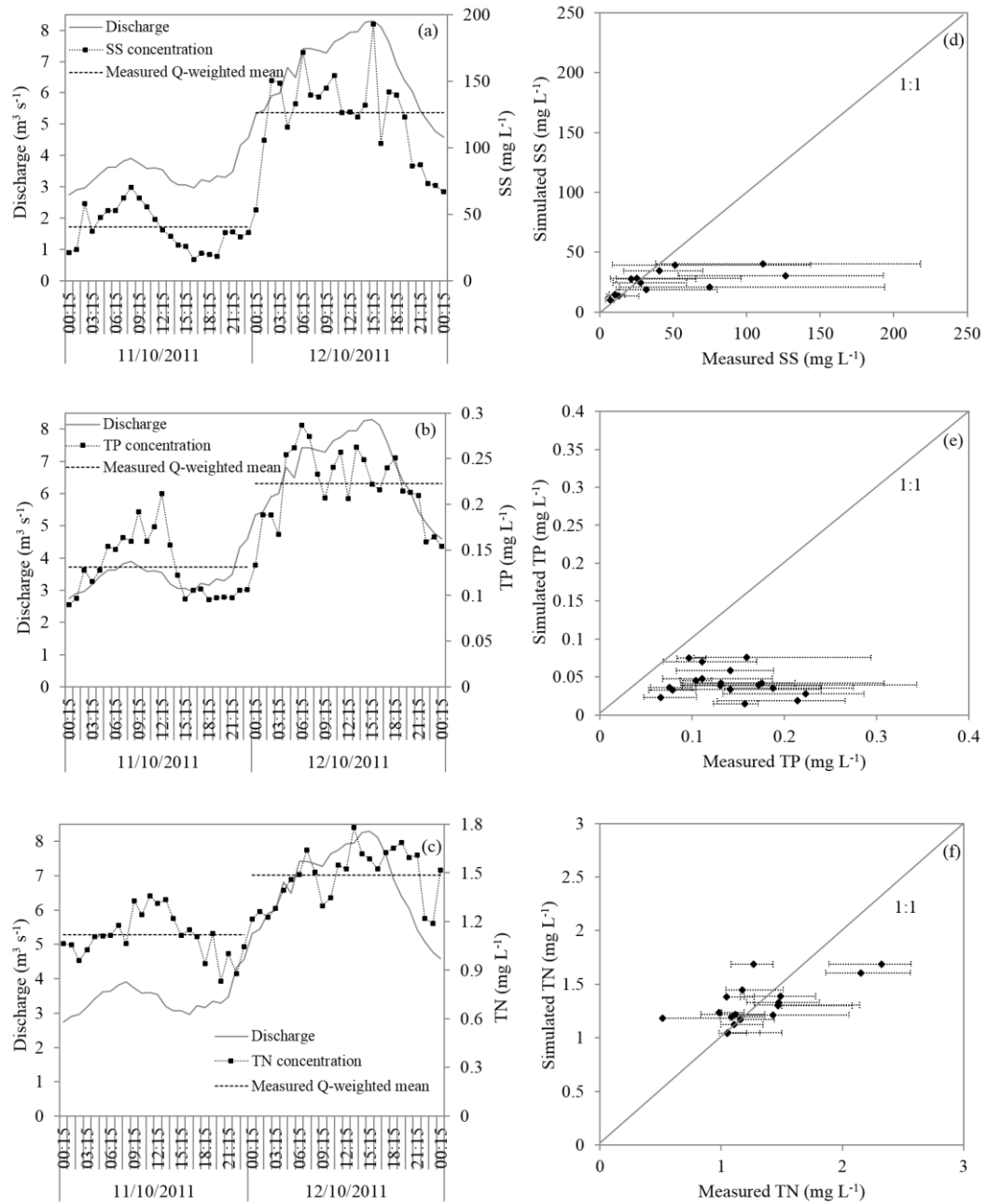
1
2 Figure 1. (a) Location of Puarenga Stream surface catchment in New Zealand,
3 Kaituna rain gauge, climate station and managed land areas for which
4 management schedules were prescribed in SWAT, and (b) location of the
5 Puarenga Stream, major tributaries, monitoring stream-gauges, two cold-water
6 springs and the Whakarewarewa geothermal contribution.



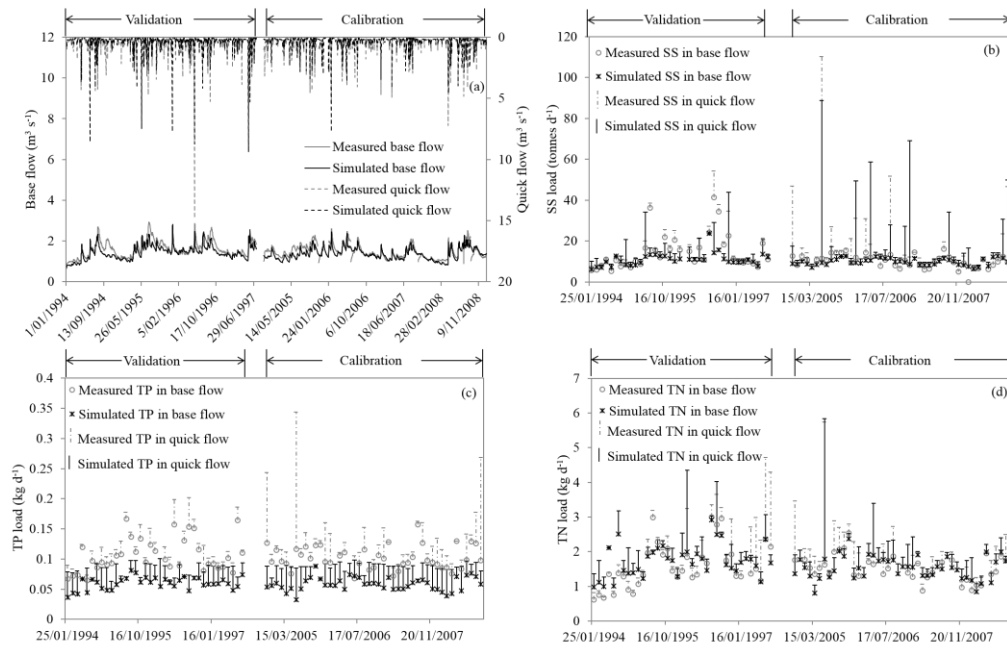
1
2 Figure 2. Flow chart of methods used to separate hydrograph and contaminant
3 loads and to quantify parameter sensitivities for: Q (discharge), SS (suspended
4 sediment), MINP (mineral phosphorus), ORGN (organic nitrogen), NH₄-N
5 (ammonium-nitrogen), and NO₃-N (nitrate-nitrogen). *NSE*: Nash-Sutcliffe
6 efficiency.



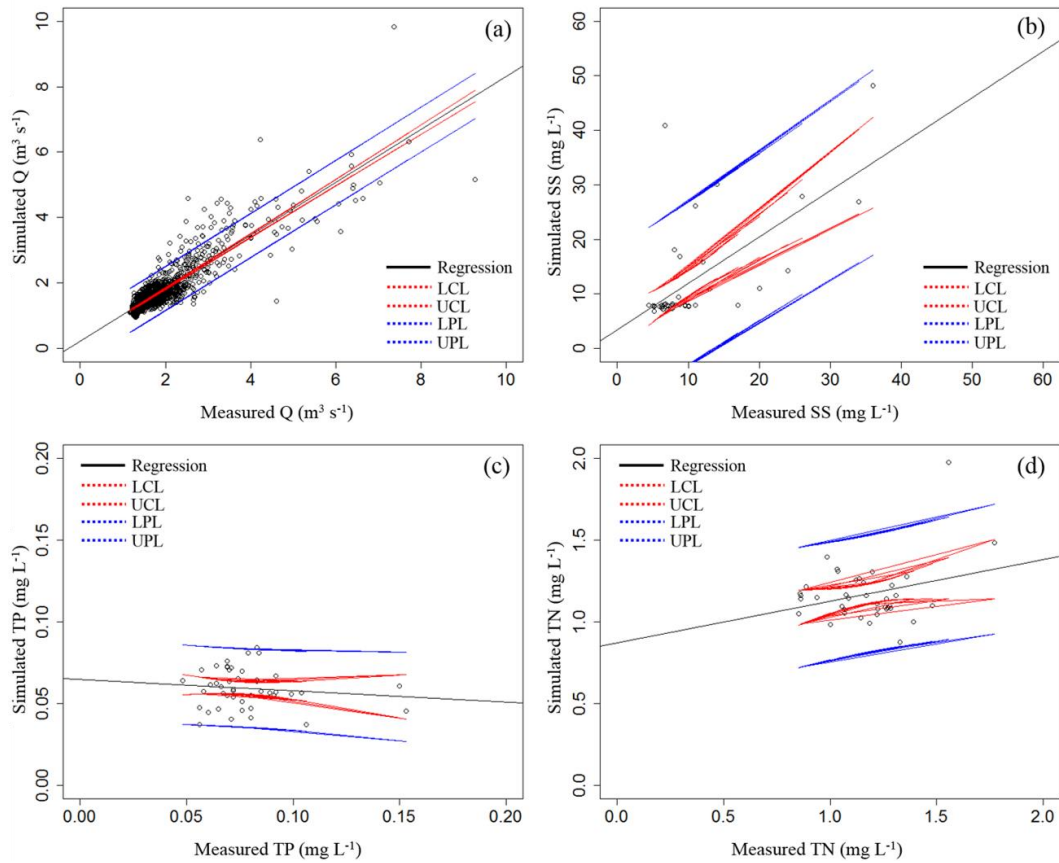
1
2 Figure 3. Measurements and daily mean simulated values of discharge, suspended
3 sediment (SS), total phosphorus (TP) and total nitrogen (TN) during calibration
4 (a–d) and validation (e–h). Measured daily mean discharge was calculated from
5 15–min observations and measured concentrations of SS, TP and TN correspond
6 to monthly grab samples.



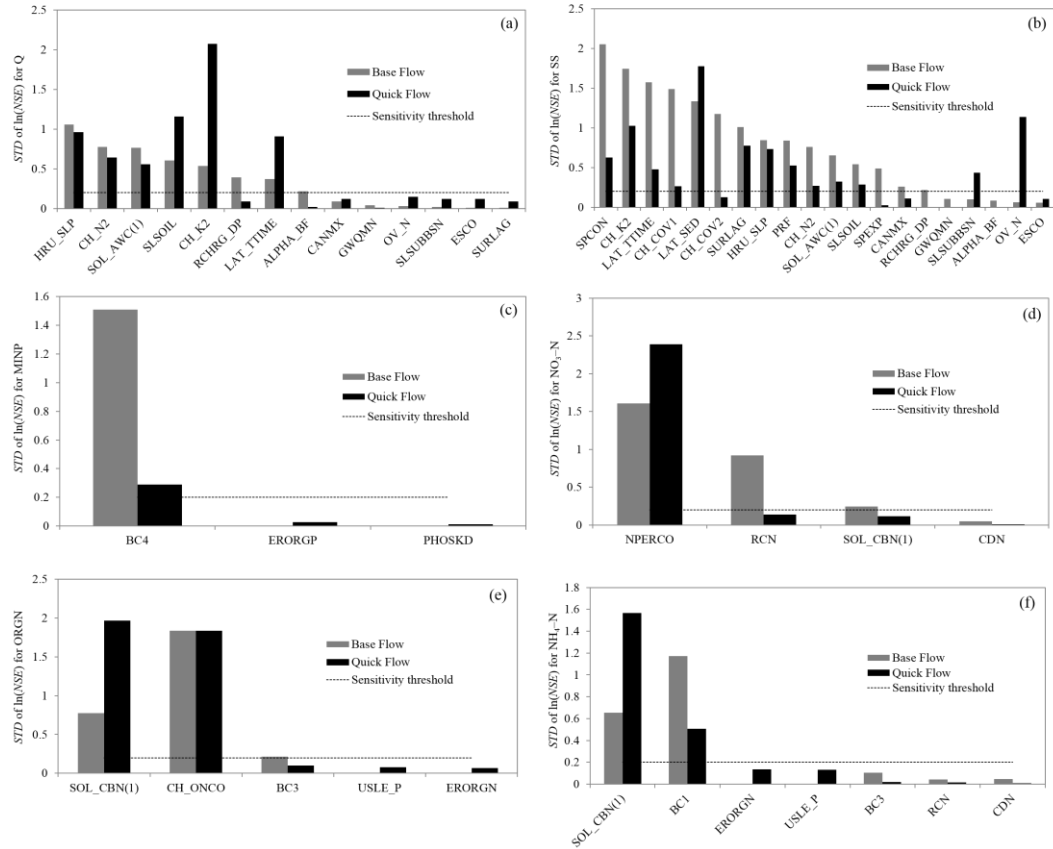
1
2 Figure 4. Example of a storm event showing derivation of discharge (Q)-weighted
3 daily mean concentrations (dashed horizontal line) based on hourly measured
4 concentrations (black dots) of suspended sediment (SS), total phosphorus (TP)
5 and total nitrogen (TN) over two days (a–c). Comparisons of Q-weighted daily
6 mean concentrations with simulated daily mean estimates of SS, TP and TN
7 (scatter plot, d–f). The horizontal bars show the ranges in hourly measurements
8 during each storm event in 2010–2012.



1
 2 Figure 5. Measurements and simulations derived using the calibrated set of
 3 parameter values. Data are shown separately for base flow and quick flow. (a)
 4 Daily mean base flow and quick flow; (b) suspended sediment (SS) load; (c) total
 5 phosphorus (TP) load; (d) total nitrogen (TN) load. Vertical lines in b–d show the
 6 contaminant load in quick flow. Time series relate to calibration (2004–2008) and
 7 validation (1994–1997) periods (note time discontinuity). Measured instantaneous
 8 loads of SS, TP, and TN correspond to monthly grab samples.



1
 2 Figure 6. Regression of measured and simulated (a) discharge (Q), concentrations
 3 of (b) suspended sediment (SS), (c) total phosphorus (TP), and (d) total nitrogen
 4 (TN) including lower and upper 95% confidence limits (LCL and UCL) and lower
 5 and upper 95% prediction limits (LPL and UPL). Note that the “choppy” shape of
 6 confidence limits shown in figures b–d were resulted from the few data points (<
 7 50) in the regressions of measured and simulated SS, TP and TN concentrations.



1
 2 Figure 7. The standard deviation (STD) of the ln-transformed Nash–Sutcliffe
 3 efficiency (NSE) used to indicate parameter sensitivity based on one-at-a-time
 4 (OAT) sensitivity analysis for separate base and quick flow components: (a) Q
 5 (discharge); (b) SS (suspended sediment); (c) MINP (mineral phosphorus); (d)
 6 $\text{NO}_3\text{-N}$ (nitrate–nitrogen); (e) ORGN (organic nitrogen); (f) $\text{NH}_4\text{-N}$ (ammonium–
 7 nitrogen). A median value (0.2) derived from the STD of ln-transformed NSE was
 8 chosen as a threshold above which parameters were deemed to be ‘sensitive’.
 9 Definitions of each parameter are shown in Table 3.